Universidad de Navarra

Facultad de Ciencias

Exploiting SR-B1 for the development of new immunotherapeutic drugs

Shirley Mireya Tenesaca Cayambe

2020

This work has been funded by The Government of Navarra

Record: 0011-1408-2016-000002

Universidad de Navarra

Memoria presentada por Dª Shirley Mireya Tenesaca Cayambe para aspirar al grado de Doctor por la Universidad de Navarra

El presente trabajo ha sido realizado bajo nuestra dirección en el Programa de Inmunología e Inmunoterapia del Cima Universidad de Navarra y autorizo su presentación ante el Tribunal que lo ha de juzgar.

Pamplona, Enero de 2020.

Dr. Pedro Berraondo

Dr. Ignacio Melero

“Nada en este mundo debe ser temido, solo entendido. Ahora es el momento de comprender más, para que podamos temer menos”.

Marie Curie

AGRADECIMIENTOS

La realización de esta tesis demandó la inversión de un tiempo valioso de muchas personas, así como del acuerdo de un equipo. El tiempo que se pasa en el laboratorio como en cualquier otro trabajo, es el tiempo en que ganas más experiencia y madurez. Queremos que la vida sea bien invertida por lo tanto nos entregamos con esfuerzo y esperamos obtener resultados excelentes. Sin embargo, la investigación es una profesión que muchas veces te hace feliz y otras veces miserable. Pienso que semeja al proyecto del hombre en la luna, tuvo que pasar varios años para su consecución, costó la vida de algunos astronautas que murieron en la explosión de su transbordador mientras apenas despegaban, pero otros pudieron pisar la luna y mirar nuestro fantástico planeta desde allí. Este trabajo es importante en mi carrera por lo tanto quiero agradecer a todas aquellas personas e instituciones que han contribuido a la elaboración de esta tesis.

Al Gobierno de Navarra por proveer la financiación, una sociedad que invierte en investigación es una sociedad que se prepara para contrarrestar sus males, crece, se convierte en líder y marca la historia de la humanidad.

A mis tutores, Kepa Berraondo e Ignacio Melero, por confiar en mi trabajo y ser los mentores de esta tesis. Les agradezco permitirme investigar, con ello aprendí de sus ideas y encaucé las mías.

A Nuria y Celia, porque han ayudado con la ejecución de varios ensayos, pienso que son el motor de este equipo.

A mis compañeras y amigas:

A Itziar, gracias por hacerme feliz en noche vieja, compartir con tu familia es el mejor acto de integración que viví.

A Lisbeth, mi amiga psicóloga, gracias por todos los momentos de reflexión, de amistad y de compartir todas nuestras ideas sobre la experiencia en el extranjero.

A Luna, Myriam, Claudia, Susy e Irene. Compartir con ustedes también me ha traído alegrías y momentos de desconexión.

A todos los compañeros de laboratorio, porque me han enseñado técnicas y protocolos para superar el desafío diario de obtener resultados. Agradezco a Mentxu, Álvaro,

Maite, Noelia, Iñaqui, Marcos, Alfonso, Rubén, etc. también al grupo de Nacho por proveer muchas veces de anticuerpos.

A Jessie y Luca, gracias por el tiempo de la estancia en Washington. Son una fuente de inspiración en mi carrera.

A mi pandilla, no cuadrilla: Araceli, Laura, Ivanka, Goretti, Alberto, Fidel, Salvador, por todos los momentos de compañía fraternal.

A mi persona favorita, Jony, creo fervientemente el proverbio que dice que somos el resultado de las personas que amamos, por tanto estoy hecha de acciones tuyas.

A mi padre, José y hermanos: Víctor, Geovanny y Jacque, gracias por apoyarme siempre con sus gestos de amor.

A mis sobrinos: Karen, Xavier, Josue, he aprendido de sus “por qué”.

INDEX

ABBREVIATIONS

LIST OF ABBREVIATIONS

$1,25(OH)_2D_3$	1,25-dihydroxyvitamin D, calcitriol, 1,25D
25(OH)D	25-hydroxyvitamin D, 25-hydroxycholecalciferol, calcifediol
25-HC	25-hydroxycholesterol
AAV	Adeno-associated viral vectors
CAMP	Cathelicidin antimicrobial peptide
CTLs	Cytotoxic T cells
CYP27B1	$25OHD_3$-1-α-hydroxylase
DCs	Dendritic cells
EAE	Experimental autoimmune encephalomyelitis
HB-EGF	Heparin-binding EGF like growth factor
HDL	High-density lipoproteins
IDO	Indoleamine-2,5-dioxygenase
IFNAR	IFN alpha/beta receptor
IFNs	Interferons
IL-10	Interleukin 10
IL-1β	Interleukin-1β
ISGs	IFN-stimulated genes
JAK	Janus kinase

LDL	Low-density lipoproteins
MHC	Major histocompatibility complex
MS	Multiple sclerosis
MVA	Modified vaccinia virus Ankara
NF-AT	Nuclear factor of activated T cells
NF-κB	Nuclear factor-κB
PD-1	Programmed death 1
SCAP	SREBP cleavage-activating protein
SR-B1	Scavenger receptor class B type 1
SREBPs	Sterol regulatory element-binding proteins
STAT	Signal transducer and activator of transcription
Th1	Type 1 T helper
TNF	Tumor necrosis factor
TYK2	Tyrosine kinase 2
VDR	Vitamin D_3 receptor
Vitamin D_3	Cholecalciferol
WT	Wild type

GENERAL INTRODUCTION

The immune system is devoted to the detection and resolution of dangerous situations in order to re-establish the homeostasis. Thus, it is highly specialized for the detection of viral or bacterial infections as well as abnormal, old, or damaged cells. The type of effector immune response depends on the damaged tissue and triggering stimuli. Four basic effector immune responses can be classified. Type 1 immune responses suppress intracellular bacteria and viruses infection. Type 2 immune responses are designed to repair damaged tissue. Type 3 responses eliminate extracellular bacteria and fungi and finally, type 4 responses are essential to exclude microorganisms in mucosae (1, 2). The immune system can also detect cancer and the adaptive and innate immune responses contribute to the prevention of tumor development. The activation of the immune system against cancer cells depends on the cell type, the inductors of the malignant transformation, the activity of stromal cells, the activity of signaling molecules such as cytokines and growth factors and the inherent immunogenicity (3).

The activity of the immune system is, therefore, an organized, balanced, and networked process. Failure of the immune responses might lead to an unrestricted response termed autoimmunity, which causes damage in the body (4). The immune system orchestration integrates stimulatory and inhibitory pathways. When an antigen is presented by major histocompatibility complex (MHC) I and II, the T-cell receptor (TCR) signaling activates effector functions in concert with a variety of co-signaling and cytokine production. This response is regulated by inhibitory factors that constitute the immune regulatory feedback mechanisms (5).

In the case of cancer, dendritic cells (DCs) present the captured antigens on MHCI and MHCII molecules to T cells, resulting in the priming and activation of effector T cell responses against the cancer-specific antigens, which migrate and infiltrate the tumor bed. There, the tumor antigen is detected through interaction between the TCR and its

cognate antigen bound to MHCI expressed on the surface of the tumor cells. This event allows for killing the cancer cells (6).

However, chronic diseases develop mechanisms to evade recognition and destruction by the effector immune cells. In cancer, tumors can evade the immune system by reducing immunogenicity, or modifying the tumor microenvironment to alter immune response (7).

Immunotherapy is a treatment intended to heal disease by stimulating or suppressing the immune system. The new generation of cancer immunotherapy relies on immune checkpoint inhibitors and T-cell adoptive therapy (8). Additionaly, other immunomodulatory drugs can produce beneficial effects in several diseases such as psoriasis, sclerosis multiple, transplantations, and lupus erythematosus.

The immune-modulating agents include, among others, cytokines such as interferons and interleukins (IL); hematopoietic growth factors such as erythropoietin, granulocyte-macrophage colony-stimulating factor and granulocyte colony-stimulating factor, Bacillus Calmette–Guérin (BCG); and biological response modifiers such as thalidomide, lenalidomide and pomalidomide (8).

In this Ph.D. project, we have exploited previous findings of the laboratory to develop new immunomodulatory drugs based on scavenger receptor class B type I (SR-B1). SR-B1 is a 509 amino acid glycoprotein containing a large extracellular domain and two transmembrane domains followed by two cytoplasmic domains. It is highly expressed in the liver and glands that secrete steroid hormones. This scavenger receptor is also present in other tissues such as brain, intestine, endothelium, and in various types of immune cells like macrophages and dendritic cells. SR-B1 has been mainly involved in lipid metabolism but this receptor also plays a dual role in inflammation. Under steady-

state conditions, SR-B1 transmits anti-inflammatory signals, but in dangerous situations, the same receptor can mediate pro-inflammatory signals (9). Thus, the activity of SR-B1 can be categorized based on the level of cytokines released upon ligand binding.

On the one hand, the ligand can be internalized and degraded without the induction of pro-inflammatory cytokines that trigger the initiation of an adaptive immune response. In such cases, the interaction between the ligand and the SR-B1 does not only lead to tolerance but also may unleash intracellular signaling that dampens other pro-inflammatory stimuli. On the other hand, the signaling mediated by SR-B1 can lead to the opposite immune reaction with the release of potent-pro-inflammatory cytokines and chemokines such as tumor necrosis factor, IL-1β, and IL-8, thus contributing to the fine-tuning of the immune response. Thus, tumor growth can be promoted by the anti-inflammatory activities of SR-B1 while anti-tumor responses can be enhanced by the pro-inflammatory activity of SR-B1 (10).

Our laboratory has demonstrated in previous studies the interaction between SR-B1 and the IFN system. SR-B1 ligands such as apolipoprotein A-1 and L37pA regulate the transcriptional response to interferon-α (IFN-α) and enhance its antiviral and antitumor activity. The effect requires the activation of toll-like receptor (TLR) 2 and TLR4 as it was annulled by the addition of anti-TLR2 or anti-TLR4 blocking antibodies. The antitumor activity of IFN-α was improved co-expressing in the liver an SR-B1 ligand and IFN-α by adeno-associated virus and eradicated liver metastases from colon cancer with reduced toxicity. This study also proved that the genetic and pharmacological inhibition of SR-B1 blocks the clathrin-dependent IFN receptor recycling pathway with a concomitant reduction in IFN-α signaling and bioactivity (11). A second study demonstrated that a high dose of an adeno-associated virus encoding IFN-α (AAV-IFN-

α) was able to eradicate a liver metastasis in a mouse model of colon cancer but induced lethal pancytopenia, but a safe dose of AAV-IFN-α was not able to eliminate them. In this IFN-α-resistant tumor model, administration of an adeno-associated vector encoding apolipoprotein A-1 fused to IFN-α was able to fully eradicate the tumor in 43% of mice without toxicity. This antitumor effect was limited by suboptimal long-term $CD8^+$ T cell activation and the expansion of T regulatory cells. In contrast, IFN-α upregulated suppressor molecules such as PD-1 and interleukin-10 on $CD8^+$ T lymphocytes (12).

In this PhD project, I have evaluated these AAV vectors in a mouse model of multiple sclerosis, a disease that will benefit from the suppressor mechanisms triggered by the sustained release of IFN-α by AAV vectors. Secondly, we developed a new screening method based on the endocytosis blockade to identify clinically available drugs that can enhance cancer virotherapy. And finally, we have extended the role of SR-B1 as a modulator of the immune system, analyzing the cross-talk of this receptor with vitamin D, which has a profound impact on cancer immune responses.

IFN-α is a cytokine approved for the treatment of several diseases. The European Medicines Agency approved interferon alfa-2b (IntronA) for the treatment of the following diseases:

1. Chronic hepatitis B in adults
2. Chronic hepatitis C, in patients aged three years and older. It is usually used in combination with ribavirin.
3. Hairy-cell leukemia

4. Chronic myelogenous leukemia in adults. IntronA can be used in combination with cytarabine (an anticancer medicine) in the first year.
5. Multiple myeloma. IntronA is used to maintain anti-cancer effects in patients who have responded to previous treatment with anticancer drugs.
6. Carcinoid tumor.
7. Malignant melanoma. IntronA is used after surgery in patients whose melanoma could come back.

The interferon beta-1b (Betaferon) was approved in patients:

1. who have experienced the signs of multiple sclerosis (MS) for the first time, and these are severe enough to justify treatment with injected corticosteroids (anti-inflammatory medicines).
2. who have MS of the type known as 'relapsing-remitting', when the patient has attacks (relapses) within periods with no symptoms (remissions), in patients with at least two relapses within the last two years.
3. who have secondary progressive MS (the type of MS that comes after relapsing-remitting MS), when their disease is active.

In spite of being an approved drug, the administration of the recombinant proteins is associated with high grade 3-4 toxicity, and therefore, new strategies to optimize the IFN-α/β are highly needed.

The second immunomodulatory molecule that we have analyzed in this Ph.D. project is vitamin D, as it has been suggested to affect the regulation of lipids directly. A recent

study identified 25-hydroxyvitamin D (25OHD) as an inhibitor of sterol regulatory element-binding protein (SREBP) activation, suggesting that 25OHD and 1,25-dihydroxyvitamin D (1,25(OH)2D3) act together to control lipogenesis. Furthermore, it has been proposed that 25OHD might work together with cholesterol and 25-hydroxycholesterol (25-HC) because 25OHD remained capable of inducing the degradation of SREBP cleavage-activating protein (SCAP) and SREBP even when SREBP activation is impaired by 25-HC or cholesterol (13). Therefore, in this Ph.D. project, we decided to study the relationship between 25OHD and SR-B1.

HYPOTHESIS AND AIMS

HYPOTHESIS

Our general hypothesis is that SR-B1 is a molecular switch that can block or enhance inflammation depending on the ligand and context. The hydrophobic areas of lipids and apolipoproteins must be hidden in lipoproteins to maintain an anti-inflammatory situation in the steady-state. But if these hydrophobic zones are exposed, they are recognized by SR-B1 as a danger signals, triggering a pro-inflammatory response. The complexity of the system has prevented the therapeutic exploitation of this receptor. Following these general hyphotesis, in this PhD thesis, we have explored three specific premises:

1. Gene therapy strategy based on the expression of sustained but low levels of IFN-α1 or IFN-α1 fused to apolipoprotein A-1 by adeno-associated viral (AAV) vectors could improve the efficacy of recombinant IFN-α-based therapies in a model of experimental autoimmune encephalomyelitis.

2. Statins could modulate the IFN-α activity and improve the antitumor immune response of modified vaccinia virus Ankara.

3. Scavenger receptor class B type I could have a role in 25-hydroxycholecalciferol cellular uptake and signaling in myeloid cells.

AIMS

1. To evaluate the efficacy and toxicity of the expression of IFN-α1 or IFN-α1 fused to apolipoprotein A-1 by AAV vectors in a model the experimental autoimmune encephalomyelitis.

2. To determine the effect of statins on the biological activity of IFN-α.

3. To enhance the antitumor activity of Modified Vaccinia Ankara encoding tumor-associated antigens by transient modulation of the IFN-α by statins.

4. To evaluate the function of scavenger receptor class B type 1 in 25-hydroxycholecalciferol biology in myeloid cells.

RESULTS

Chapter 1: “Treatment of Experimental Autoimmune Encephalomyelitis by Sustained Delivery of Low-Dose Interferon alpha”

Title

Treatment of experimental autoimmune encephalomyelitis by sustained delivery of low-dose interferon alpha

Authors

Marcos Vasquez[1,2], Marta Consuegra-Fernández[4,5,6], Fernando Aranda[4,5,6], Aitor Jimenez[1], Shirley Tenesaca[1,2], Myriam Fernandez-Sendin[1,2], Celia Gomar[1,2], Nuria Ardaiz[1,2], Noelia Casares[1,2], Juan José Lasarte[1,2], Francisco Lozano[4,5,6], Pedro Berraondo[1,2,3]

Affiliations

[1]Program of Immunology and Immunotherapy, Center for Applied Medical Research (CIMA), Pamplona, Spain

[2]Navarra Institute for Health Research (IDISNA), Pamplona, Spain

[3]Centro de Investigación Biomédica en Red de Cáncer (CIBERONC), Spain.

[4]Institut d'Investigacions Biomédiques August Pi i Sunyer (IDIBAPS), Barcelona, Spain.

[5]Servei d'Immunologia, Hospital Clínic de Barcelona, Barcelona, Spain.

[6]Departament de Biomedicina, Universitat de Barcelona, Barcelona, Spain.

Abstract

Multiple sclerosis (MS) is a chronic autoimmune disease with no curative treatment. The immune regulatory properties of type I interferons have led to the approval of interferon beta (IFN-β) for the treatment of relapsing-remitting MS. However, there is still an unmet need to improve the tolerability and efficacy of this therapy. In this work, we evaluated the sustained delivery of interferon-alpha 1 (IFN-α), either alone or fused to apolipoprotein A-1 (IFN-α/ApoA1) by means of an adeno-associated viral (AAV) system in the mouse model of myelin oligodendrocyte glycoprotein (MOG)-induced experimental autoimmune encephalomyelitis (EAE). These in vivo experiments demonstrated the prophylactic and therapeutic efficacy of the AAV-IFN-α or AAV-IFN-α/ApoA1 vectors in EAE, even at low doses devoid of hematological or neurological toxicity. The sustained delivery of such low-dose IFN-α resulted in immunomodulatory effects, consisting of pro-inflammatory monocyte and T regulatory cell (Treg) expansion. Moreover, encephalitogenic T lymphocytes from IFN-α treated mice re-exposed to the MOG peptide in vitro showed a reduced proliferative response and cytokine (IL-17A and IFN-γ) production, in addition to up-regulation of immunosuppressive molecules such as IL-10, IDO or PD-1. In conclusion, the results of the present work support the potential of sustained delivery of low-dose IFN-α for the treatment of MS and likely other T-cell dependent chronic autoimmune disorders.

Introduction

Multiple sclerosis (MS) is a chronic autoimmune inflammatory disease that affects the central nervous system and is characterized by inflammation, demyelination, and axonal loss. The etiopathogenesis of MS remains incompletely understood, as a result of the complex interplay between several genetic, environmental and infectious factors (14).

Although there is still no effective therapy for MS, Interferon β (IFN-β) has been at the forefront of therapeutic options for many years, and is widely used as first-line treatment for the disorder (15). IFN-β belongs to the type I interferon group, which includes IFN-α (with 13 subtypes), IFN-β, IFN-ε, IFN-κ, and IFN-ω in humans. They are pleiotropic cytokines synthesized and released from different cell sources upon danger signal delivery following host-pathogen interactions, and display antiviral, antiproliferative and immunomodulatory activities (16). Based on the latter properties of type I IFNs, IFN-β has been widely used for the treatment of MS (17). Additionally, IFN-α has also shown therapeutic activity in MS patients by reducing brain lesions, as assessed by magnetic resonance imaging (MRI), and attacks (17-20). IFN-α and IFN-β bind to the IFNAR1/2 and activate the JAK/STAT signaling pathway. Although both type I IFNs show some differences at the cellular level (21), they display a similar clinical efficacy and therefore, the rationale behind the treatment of MS patients with IFN-β instead of using IFN-α is a mix of scientific evidence and tradition.

T-cells play a critical role in the etiopathogenesis of MS (22). Indeed, autoreactive T cells from the helper-1 (Th1), helper-17 (Th17), γδ, and CD8+ subsets, have been implicated in the accompanying inflammation and neurodegeneration. Cytokines released from Th1 and Th17 cells contribute to enhance Major Histocompatibility

Complex (MHC) class II expression on antigen-presenting cells and increase the cytotoxic activity of autoreactive CD8, macrophages and Natural Killer cells (NK). Moreover, Th17 cells seem to be the main driver in the pathogenesis of MS (23).

In contrast, Th2 cytokines are associated with anti-inflammatory effects. In this setting, regulatory T cells (Treg) can inhibit the activity of autoreactive T cells (24). It has been demonstrated that Treg depletion by using anti-CD25 antibodies, enhanced severity of symptoms in an experimental autoimmune encephalomyelitis (EAE) model of MS by a mechanism that involves interleukin 10 (IL-10) (25). In addition, adoptive cell transfer of Treg conferred significant protection (26).

The mechanisms of action of type I interferons in MS are complex and involve effects at multiple levels. Type I interferons may reduce the trafficking of inflammatory cells across the blood-brain barrier, induce apoptosis of autoreactive T-cells, increase the levels of anti-inflammatory cytokines (IL-10, IL-4), decrease the levels of pro-inflammatory cytokines (IL-17, IFN-γ, TNF-α), and modulate the function of Treg (27).

Several clinical trials have demonstrated that the clinical benefits of IFN-β in MS are dose-dependent (28). The highest doses required to achieve clinical efficacy are, however, normally associated with increased side effects and lead to the production of neutralizing antibodies (29). Additionally, its therapeutic efficacy depends on frequent/repeated administration to sustain optimal levels of its biological effect (30). Clinical studies performed in healthy voluntaries and MS patients have demonstrated that IFN-β given every other day had significantly greater overall biological activity (31-33) and therapeutic effect (34-36) than weekly administration. Thus, the safety and efficacy of IFN-based therapies may be improved with new administration schedules or IFN delivery systems.

To further improve the pharmacokinetic properties of IFN-based therapies, we have developed a strategy based on IFN-α1 expression by adeno-associated viral (AAV) vectors (12). The low immunogenicity, lack of pathogenicity, persistence and long-term expression of the transgene incorporated into AAV, makes this vector a suitable tool for this approach. Moreover, several clinical trials have demonstrated the safety and efficacy of AAV (37). Additionally, we have developed a strategy based on the fusion of IFN-α1 to apolipoprotein A-1 (IFN-α/ApoA1) (38). This fusion protein presents a longer half-life in circulation with no systemic toxicity when high doses of the AAVs are administered for oncotherapeutic purposes (12).

Herein, we evaluated the therapeutic activity of sustained AAV-mediated IFN-α or IFN-α/ApoA1 expression in EAE mice. We demonstrated that long-term exposure to low IFN-α or IFN-α/ApoA1 levels is sufficient to safely prevent and control EAE symptoms in mice by reducing inflammatory infiltrates, tissue damage and cytokine responses.

Material and methods

Animal Handling

In vivo experiments were performed in 6-8 week-old female C57BL/6 mice (~20 g) purchased from Harlan Laboratories (Barcelona, Spain). The mice were maintained under specific-pathogen-free conditions, and the experimental design was approved by the ethics committees for animal testing of University of Barcelona and Universidad de Navarra.

Induction and clinical score of EAE

Anesthetized mice were immunized by subcutaneous injection of 150 µg of Myelin oligodendrocyte glycoprotein peptide 35-55 (MOG_{35-55}, MEVGWYRSPFSRVVHLYRNGK; GenScript, Piscataway, NJ) dissolved in 100 µl of PBS and emulsified with 100 µl of complete Freund's adjuvant (Difco, Detroit, MI, USA) containing 1 mg *Mycobacterium tuberculosis* H37RA (#231131; BD Biosciences). Each mouse received 100 µl of the emulsion per flank. Intraperitoneal (*i.p.*) doses of 500 ng of Pertussis toxin (Sigma-Aldrich, St Louis MO) dissolved in PBS were administered at the time of immunization and 48 h later. Animal weight and clinical score were analyzed daily as follows: 0 = no clinical signs, 0.5 = partial flaccid paralysis of the tail, 1 = flaccid paralysis of the tail, 2 = weak hind leg paralysis, 3 = bilateral hind leg paralysis, 4 = hind and foreleg paralysis, 5 = moribund, 6 = death.

Recombinant AAVs were administered once retro-orbitally in a total volume of 200 µl. Previously, animals were anesthetized by *i.p.* injection of a 1:9 (v/v) mixture of xylazine (Rompun 2%, Bayer) and ketamine (Imalgene 500, Merial).

Recombinant mouse IFN-α produced in CHO cells was purchased from Hycult Biotech (Uden, Netherlands). 10,000 units were administered via the *retroorbital* route three times per week .

To analyze the encephalitogenic capacity of spleen cells isolated from AAV-GFP or AAV-IFN-α, mice were immunized and treated with the AAV vectors four days later. At day 15, donor mice were sacrificed and splenocytes cultured in complete RPMI at 37ºC and 5% CO_2 in the presence of 20 μg/ml MOG_{35-55}, 20 ng/ml recombinant mouse interleukin 12 (Peprotech, London, UK) and 10 μg/ml anti-mouse IFNγ antibody (XMG1.2, BioXCell, West Lebanon, NH). Three days later, $10x10^6$ cells were inoculated by retroorbital administration to 10 week-old female C57BL/6 mice. Animal weight and clinical score were analyzed daily.

Production of recombinant AAV vectors

AAV serotype 8 vectors were constructed to express IFN-α, IFN-α/ApoA1 or GFP under the transcriptional control of the elongation factor 1α promoter. AAV vectors were produced by co-transfection of the plasmids pDP8.ape (PlasmidFactory GmbH & Co. KG, Bielefeld Germany) and pAAV encoding IFN-α1, IFN-α/ApoA1(26) or GFP into HEK-293T cells. For each production, a mix of 20 μg of pAAV, 55 μg of pDP8.ape and linear PEI “MAX” 25 kDa (Polysciences, Warrington, PA, USA) was transfected into HEK-293T cells. Forty-eight hour later, AAV were isolated from the cell lysates by ultracentrifugation in Optiprep Density Gradient Medium (Sigma-Aldrich, St Louis MO) and viral DNA was isolated using “The High Pure Viral Nucleic Acid” kit (Roche Applied Science. Mannheim, Germany). The titers of viral particles were subsequently

determined by real-time quantitative PCR using primers specific to the EF promoter: Fw: 5'-ggtgagtcacccacacaaagg-3' and Rv: 5'-cgtggagtcacatgaagcga-3'.

Cell isolation

Spleen cell suspensions were obtained in cold RPMI 1640 by mechanically disrupting the tissue through a 70 μm nylon cell strainer (Falcon, Becton Dickinson Labware) with a syringe plunger. Red blood cells were removed using Ammonium-Chloride-Potassium (ACK) lysis buffer (Gibco BRL, Rockville, MD, USA).

$CD4^+CD25^+$ cells were enriched from pooled spleen by anti-mouse FITC-conjugated $CD4^+$ and APC-conjugated $CD25^+$ mAbs (ebioscience, CA, USA) and purified by FACSAriaII cell sorter (BD Biosciences).

ELISA

Serum IFN-α levels were quantified with VeriKine™ Mouse Interferon Alpha ELISA Kit (PBL, NJ, USA) following the manufacturer's recommendations. The levels of IFN-γ and IL-17A in the supernatant of splenocytes stimulated with MOG_{35-55} peptide were measured using Mouse IL-17A ELISA Ready-SET-Go! (eBioscience, San Diego, CA) and BD OptEIA™ - Mouse IFN-γ ELISA Set (BD Bioscience) kits respectively and according to the manufacturer's recommendations.

Hemogram

Blood samples were collected on day 52 after immunization in tubes with 0.5% heparin (Mayne Pharma, Mulgrave, Australia) as the final concentration. Hemograms were

analyzed using the Drew Scientific HemaVet Hematology Analyzer (CDC Technologies, Oxford, CT) following the manufacturer's recommendations.

RNA isolation and quantification of mRNA

RNA was isolated from total and sorted $CD4^+CD25^+$ splenocytes or spinal cords using the Maxwell® 16 Total RNA Purification Kit (Promega, Madison, Wisconsin, USA), quantified in a NanoDrop spectrophotometer (Thermo Scientific, Wilmington, USA), and retrotranscribed (500 ng) to cDNA with Moloney murine leukemia virus (M-MLV) reverse transcriptase from Promega, according to the manufacturer's instructions.

Quantitative real-time PCR (qRT-PCR) was performed with iQ SYBR Green Supermix (Bio-Rad) using specific primers for: IFN-stimulated gene 15 (Isg15, 5'-gattgcccagaagattggtg-3' and 5'-tctgcgtcagaaagacctca-3'), Ubiquitin specific peptidase 18 (Usp18, 5'-ccaaaccttgaccattcacc-3' and 5'-atgaccaaagtcagcccatcc-3'), 2'-5'-oligoadenylate synthetase (2'5'Oas, 5'-actgtctgaagcagattgcg-3' and 5'-tggaactgttggaagcagtc-3'), Interleukin 10 (IL-10, 5'-ggacaacatactgctaaccg-3' and 5'-aatcactcttcacctgctcc-3'), Indoleamine 2,3-Dioxygenase 1 (Ido, 5'-ccttgaagaccaccacatag-3' and 5'-agcacctttcgaacatcgtc-3'), Programmed cell death protein 1 (PD-1, 5'-actggtcggaggatcttatg-3' and 5'-atcttgttgaggtctccagg-3'), Cluster of differentiation 4 (CD4, 5'-gaacatctgtgaaggcaaag-3' and 5'-cagcagcagcagcagcaag-3'), Forkhead box P3 (Foxp3, 5'-gtttctcaagcactgccaag-3' and 5'-tgtggaagaactctgggaag-3'), Interferon gamma (IFN-γ, 5'-tcaagtggcatagatgtggaa-3' and 5'-tggctctgcaggattttcatg-3'), Interleukin 17A (IL-17A, 5'-ctgtgtctctgatgctgttg-3' and 5'-tatcagggtcttcattgcgg-3'), F4/80 antigen (F4/80, 5'-cccagcttctgccacctgca-3' and 5'-ggagccattcaagacaaagcc-3'), and Ribosomal Protein, Large, P0 (RPLP0, 5'-aacatctccccttctcctt-3' and 5'-gaaggccttgacctttcag-3').

As RPLP0 levels remained constant across different experimental conditions, this parameter was used to standardize gene expression. The amount of each transcript was expressed by the formula $2^{\Delta Ct}$ ($2^{ct(RPLP0) - ct(gene)}$), with ct being the point at which the fluorescence rises significantly above the background levels.

Splenocyte proliferation assays

Splenocytes (1 x 10^5) were cultured in 96-well plates for 48 h with MOG_{35-55} (50 µg/ml). During the last 12 h, samples were pulsed with 0.5 µCi of [^{3}H]-thymidine and harvested with a Micro Beta Filter Mate-96 harvester (Perkin Elmer). [^{3}H]-thymidine incorporation was measured using an automated Topcount liquid scintillation counter (Packard).

Flow cytometry analyses

Flow cytometry analyses were performed using a FACS Canto II flow cytometer (BD Biosciences). Splenocytes (5 x 10^5) were stained with anti-mouse APC-conjugated CD11b (M1/70; BioLegend), PE-conjugated Ly6G (1A8; BD Bioscience) and FITC-conjugated Ly6C (AL-21; BD Bioscience), for 15 min at 4 °C in FACS buffer (PBS plus 5% fetal bovine serum, and 2.5 mM EDTA), and then washed twice and suspended in the same buffer for further flow cytometric analysis. For Treg cell analyses, splenocytes were stained with FITC-conjugated CD4 (RM4-5; eBioscience), APC-conjugated CD25 (PC61.5, eBioscience) and PE-conjugated FoxP3 (FJK-16s; eBioscience) mAbs.

For intracellular IFN-γ and IL-17A cytokine stainings, splenocytes (5 x 10^5) were stimulated with MOG_{35-55} (50 µg/ml) for 66 h. During the last 6 h, cells were re-stimulated with the same amount of MOG_{35-55} plus GolgiPlug (1 µl/mL; BD Bioscience), stained with PE-conjugated CD4 (RM4-5; BD Bioscience) mAb for 15 min at 4°C, and fixed with Cytofix/Cytoperm solution (BD Bioscience) for 20 min at 4°C. Finally, cells were stained with PE/Cy7-conjugated anti-mouse IL-17A (TC11-18H10; BioLegend) and FITC-conjugated anti-mouse IFN-γ (XMG1.2; BioLegend) respectively for 30 min at 4°C, washed twice and suspended in FACs buffer prior to flow cytometry analysis.

Histological analyses

At day 21 post-immunization, mice (n = 4/group) were euthanized and their spinal cords isolated and fixed in 4% of paraformaldehyde for 24 h. The fixed samples were washed with PBS and stored in 70% ethanol at room temperature until processing. Cell infiltration and myelination were analyzed histochemically by H&E and Luxol fast blue staining respectively. Quantification was performed by selecting white matter in spinal cord sections. Pixel intensity and density were quantified over a threshold color using Matlab software (Magnification 10X).

Tail suspension test

Mice were suspended by the tail with adhesive tape to a horizontal bar, so that the head of the mouse was 20 cm above the floor. The time of immobility was measured by direct-eye observation for 6 min. Experiments were conducted by personnel blinded to

the treatment conditions. Depression is expressed as the accumulated time of animal immobility in seconds during a 6-min test.

Statistical analyses

Statistical analyses were carried out with Prism software (GraphPad Software, Inc.). Data are usually presented as ± SD and means were compared using a student *t* test. To compare three groups, One-way ANOVA followed by Bonferroni post-test was used. Both EAE disease scores and weight curves were fitted and analyzed with nonlinear regression to a second-order polynomial (quadratic) model. The survival data were represented in Kaplan-Meier graphs and analyzed using the log-rank test to determine levels of significance. p values < 0.05 were considered significant.

Results

AAVs encoding IFN-α or IFN-α fused to apolipoprotein A-1 prevents EAE symptoms

Recombinant AAV vectors were used *in vivo* to evaluate whether sustained doses of IFN-α1 or IFN-α/ApoA1 could protect mice from EAE. To this end, high-dose AAVs (5 x 10^{11} viral genomes (vg)/mouse) were administered two days prior to EAE induction (Figure 1A). All mice receiving control AAV-GFP developed EAE symptoms, while those receiving AAV-IFN-α or IFN-α/ApoA1 showed mild or even no symptoms at all (Figure 1B and 1C). However, mice treated with AAV-IFN-α died likely because of the hematological toxicity usually associated with the high and sustained doses of this cytokine(24). All mice treated with AAV-IFN-α/ApoA1 survived (Figure 1D).

The next step was to investigate whether lower doses of AAV-IFN-α could protect against EAE development without inducing fatal toxicity. Accordingly, decreasing doses of the AAV-IFN-α ($5x10^{11}$, $1x10^{11}$ and $1x10^{10}$ vg/mouse) were administered 2 days before MOG immunization. As illustrated by Figures 1E-1F, all three tested doses protected mice from developing EAE but, importantly, all animals survived only when the lowest dose ($1x10^{10}$ vg/mouse) was used (Figure 1G).

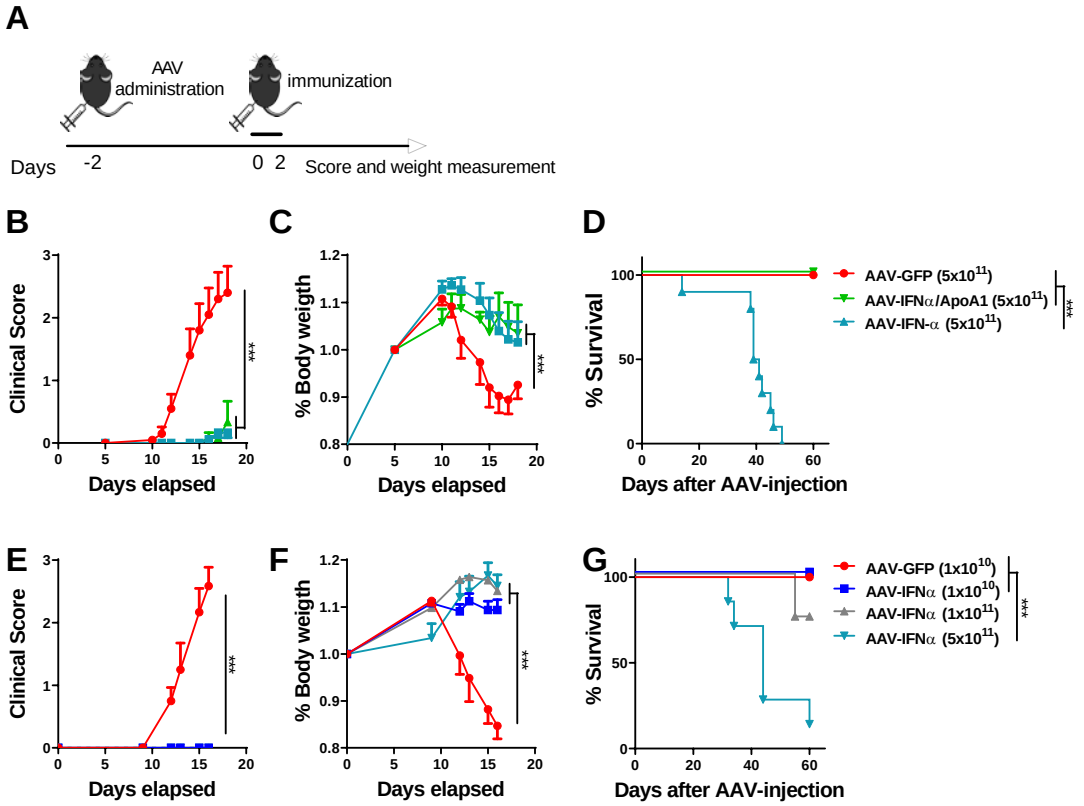

Figure 1. Sustained doses of IFN-α or IFN-α/ApoA1 prevent the onset of clinical signs of EAE in mice. C57BL/6 (n = 6 per group) mice were treated with high-dose ($5x10^{11}$ vg) AAVs encoding GFP, IFN-α or IFN-α/ApoA1 two days before MOG immunization **(A-D)**, and clinical score **(B)**, body weight **(C)** and survival **(D)** were further determined. Decreasing doses of AAV-IFN-α ($5x10^{11}$, $1x10^{11}$, and $1x10^{10}$ vg) were administered to C57BL/6 mice (n = 6 per group) two days before MOG immunization **(E-G)**, and clinical score **(E),** body weight **(F)** and survival **(G)** were further determined. Data from the clinical score and weight curves are expressed as mean ± SEM and analyzed by extra sum-of-squares F test, ***$p < 0.001$. Survival is represented by a Kaplan–Meier plot (Log-rank test. ***p < 0.001).

AAVs encoding IFN-α or IFN-α fused to apolipoprotein A-1 protect from ongoing EAE disease

Although the AAV8-mediated transgene expression reaches its peak at two weeks after administration(27), we decided to evaluate the use of therapeutic and safe doses of AAVs encoding IFN-α or AAV-IFN-α/ApoA1 in mice undergoing EAE. To this end, mice were treated with the lowest AAV-IFN-α dose ($1x10^{10}$ vg/mouse) four days after MOG-immunization (Figure 2A). As shown in Figure 2B and 2C, they all were almost completely protected from EAE. Mice treated with a safe AAV-IFN-α/ApoA1 dose ($5x10^{11}$ vg/mouse) developed EAE, but symptom severity scores were significantly lower than with control AAV-GFP (Figure 2B and 2C). Interestingly, the clinical course of EAE declined by two weeks after virus AAV-IFN-α/ApoA1 administration when maximum AAV expression levels are expected. In this experimental setting, the administration of 10,000 units of recombinant mouse IFN-α three times per week does not improve the clinical symptoms (Figure 2D and 2E).

We next decided to evaluate the therapeutic efficacy of the viruses once the disease had been fully developed. To this end, similar AAVs doses as above were administered when the average symptom severity scores reached ~2 (day 13) (Figure 2F). As shown in Figures 2G and 2H, mice treated with AAV-IFN-α or AAV-IFN-α/ApoA1 displayed a significant sharp decline in the clinical signs of the disease as compared to the control group.

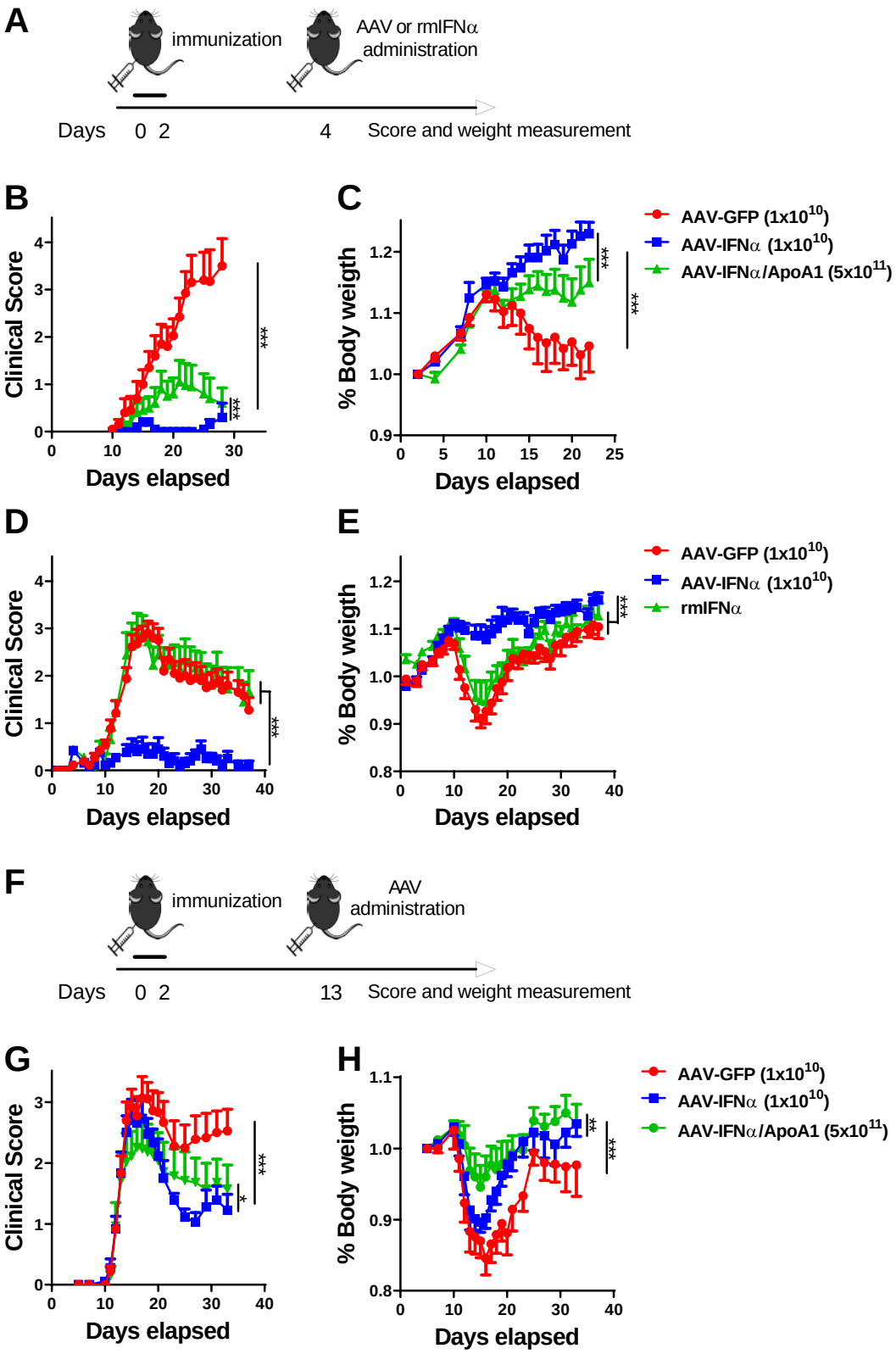

Figure 2. Therapeutic administration of IFN-α or IFN-α/ApoA1 reduces the onset of clinical signs of EAE in mice. AAVs encoding GFP, IFN-α or IFN-α/ApoA1 or

recombinant mouse IFN-α (rmIFN-α) were administered to C57BL/6 mice (n = 12 per group) at day four after immunization **(A-E)**. The clinical score **(B)** and body weight **(C)** of mice receiving AAVs encoding GFP ($1x10^{10}$ vg), IFN-α ($1x10^{10}$ vg) or IFN-α/ApoA1($5x10^{11}$ vg) were recorded over time. For evaluation purposes, the clinical score **(D)** and body weight **(E)** of mice receiving the above mentioned doses of AAVs encoding GFP and IFN-α were compared with those administered with 10,000 units of rmIFN-α i.v. three times per week (n = 13 per group). In another set of experiments (**F-H**), the clinical score **(G)** and body weight **(H)** of mice (n = 9 per group) administered with AAVs encoding GFP ($1x10^{10}$ vg), IFN-α ($1x10^{10}$ vg) or IFN-α/ApoA1($5x10^{11}$ vg) thirteen days after immunization and once the mean of clinical scores reached an average of two (day 13) were determined. Data from the clinical score and weight curves are expressed as mean ± SEM and analyzed by extra sum-of-squares F test, ****p < 0.001*.

Therapeutic dose of AAV-IFN does not induce hematological or neurological toxicity

Next, we analyzed the advent of putative adverse effects following a therapeutic dose of $10x10^{10}$ vg AAV-IFN-α four days after EAE induction. On day 52 after immunization, analysis of peripheral blood cells showed no differences regarding platelet and erythrocyte between untreated mice and the AAV-IFN-α treated mice (Figure 3A), which is indicative of absent hematologic toxicity of the selected AAV dose. However, circulating leukocytes were reduced in the AAV-IFN-α treated group, likely reflecting the known up-regulation of CD69 expression and the subsequent retention in secondary lymphoid organs induced by IFN-α (28) (Figure 3A). To analyze the neurological toxicity, we determined the cytokine-mediated depression using the tail suspension test at day 40 after immunization. No differences in the immobility time were detected in mice treated with AAV-GFP or AAV-IFN-α (Figure 3B).

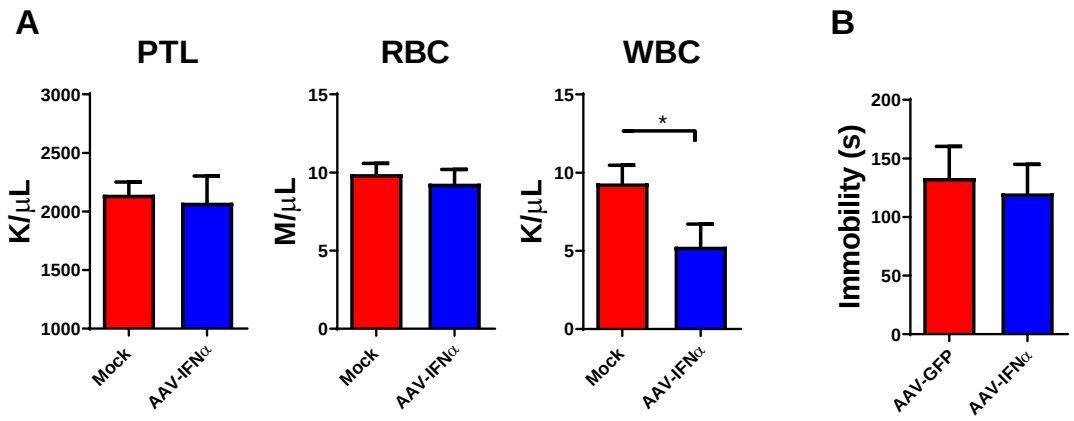

Figure 3. Long-term exposure to low-dose IFN-α does not induce hematological or neurological toxicity. C57BL/6 mice were immunized and treated with AAV-IFN-α four days later. **(A)** White blood cells (WBC), platelets (PLT) and red blood cells (RBC) were quantified from peripheral blood at day 52 after immunization (n = 4, mice per group). **(B)** Immobility time in a 6-min tail suspension test (n = 10 per group). Data are expressed as mean + SD. (t-test. *$p < 0.05$).

Activity of sustained low dose IFN-α on immune cells

Low-dose ($1x10^{10}$ vg/mouse) AAV-IFN-α was safe and effectively controlled the disease progression, and allowed detectable circulating levels of IFN-α at 3 weeks post-AAV-IFN-α administration (Figure 4A). In an attempt to figure out the mechanism of action of this vector dose, we first analyzed the surface expression level of Ly6C -a glycosylphosphatidylinositol-linked protein expressed by inflammatory monocytes(29) and considered a biomarker of IFN-α activity (30). As shown by Figure 4B and Supplemental Fig. 1, Ly6C was upregulated in monocyte populations ($Ly6G^{-}CD11b^{+}$) of WT mice treated with AAV-IFN-α. In EAE mice, Ly6C was also up-regulated by

AAV-IFN-α but also control AAV-GFP, reflecting the on-going inflammatory process (Figure 4B). Next, the percentages of spleen Treg cells were found higher in both the WT and the EAE mice treated with AAV-IFN-α compared with the AAV-GFP control group (Figure 4C and Supplemental Fig. 2). To confirm that IFN-α was the major driver of Treg expansion in the immunized group, and that this population responded to the low concentration of IFN-α in circulation, $CD4^+CD25^+$ were isolated, and the levels of different IFN-stimulated genes (ISGs) were assessed. The amounts of the ISG transcripts were significantly higher in the group treated with AAV-IFN-α than in the controls, thus confirming the direct activity of IFN-α on Tregs (Figure 4D). Neutrophils, which have an important role in the pathogenesis of EAE(31), were dramatically expanded in MOG-immunized animals, and AAV-IFN-α administration reduced the disease-induced neutrophil expansion significantly (Figure 4E and Supplemental Fig. 1).

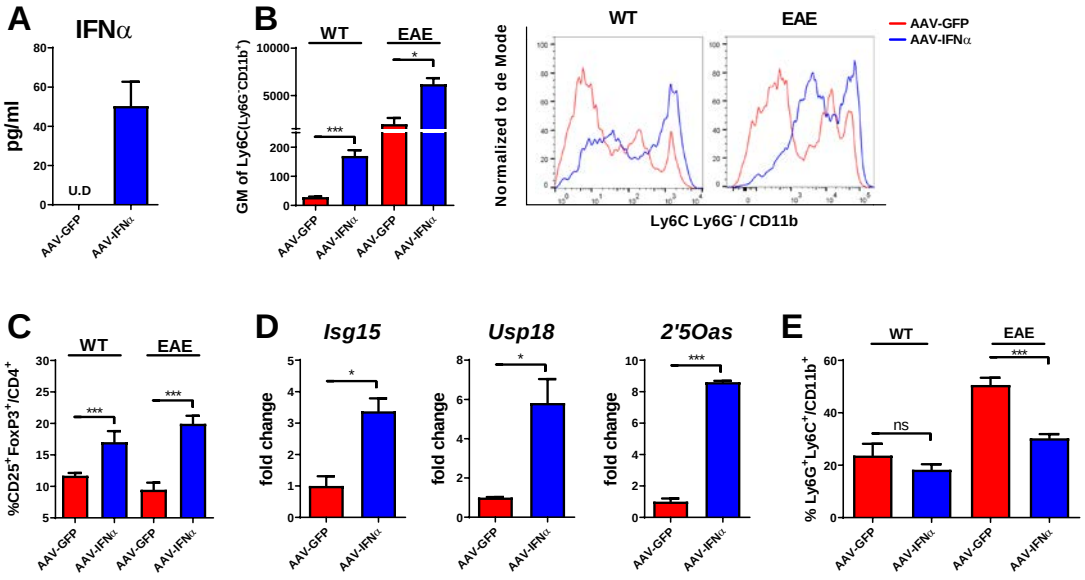

Figure 4. Characterization of the effect of sustained low-dose IFN-α on immune cells. (A) Serum IFN-α levels from C57BL/6 mice three weeks post-AAV-GFP ($1x10^{10}$ vg) or IFN-α ($1x10^{10}$ vg) administration, as determined by ELISA. **(B-E)** Analysis of

monocyte ($Ly6C^+LyG^-CD11b^+$), Treg ($CD4^+CD25^+FoxP3^+$) and neutrophil ($Ly6G^+Ly6C^+CD11b^+$) populations in spleens from mice administered with AAV-GFP ($1x10^{10}$ vg) or IFN-α ($1x10^{10}$ vg) four days after being immunized (EAE) or not (WT) with MOG. (**B,C,E**). Flow cytometry analysis showing the geometric mean (GM) of Ly6C in $Ly6G^-$ $CD11b^+$ (**B**) and the percentage of $CD25^+$ $FoxP3^+$ in CD4+ **(C)** and $Ly6G^+Ly6C^+$ in $CD11b^+$ spleen cells (**E**). **(D)** mRNA levels of different interferon-stimulated genes were quantified by quantitative real-time PCR in $CD4^+CD25^+$ cells isolated by cell sorting from spleens of EAE mice. Data are expressed as mean + SD. (t-test. *p < 0.05, ***p < 0.001).

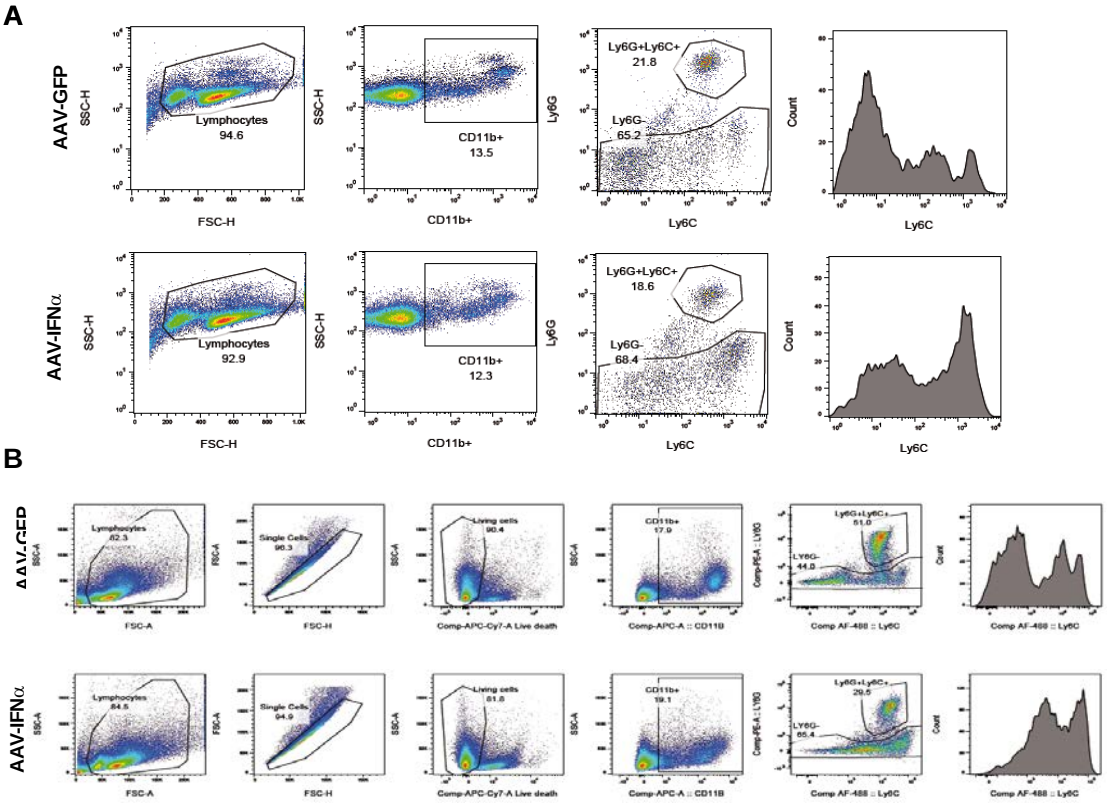

Figure S1: Gating strategy for myeloid cell analysis. Representative analysis of monocyte (Ly6C+LyG-CD11b+), and neutrophil (Ly6G+Ly6C+CD11b+) populations in spleens from mice treated with AAV-GFP (1x1010 vg) or IFN-α (1x1010 vg) four days after being mock-immunized **(A)** or immunized with MOG **(B).**

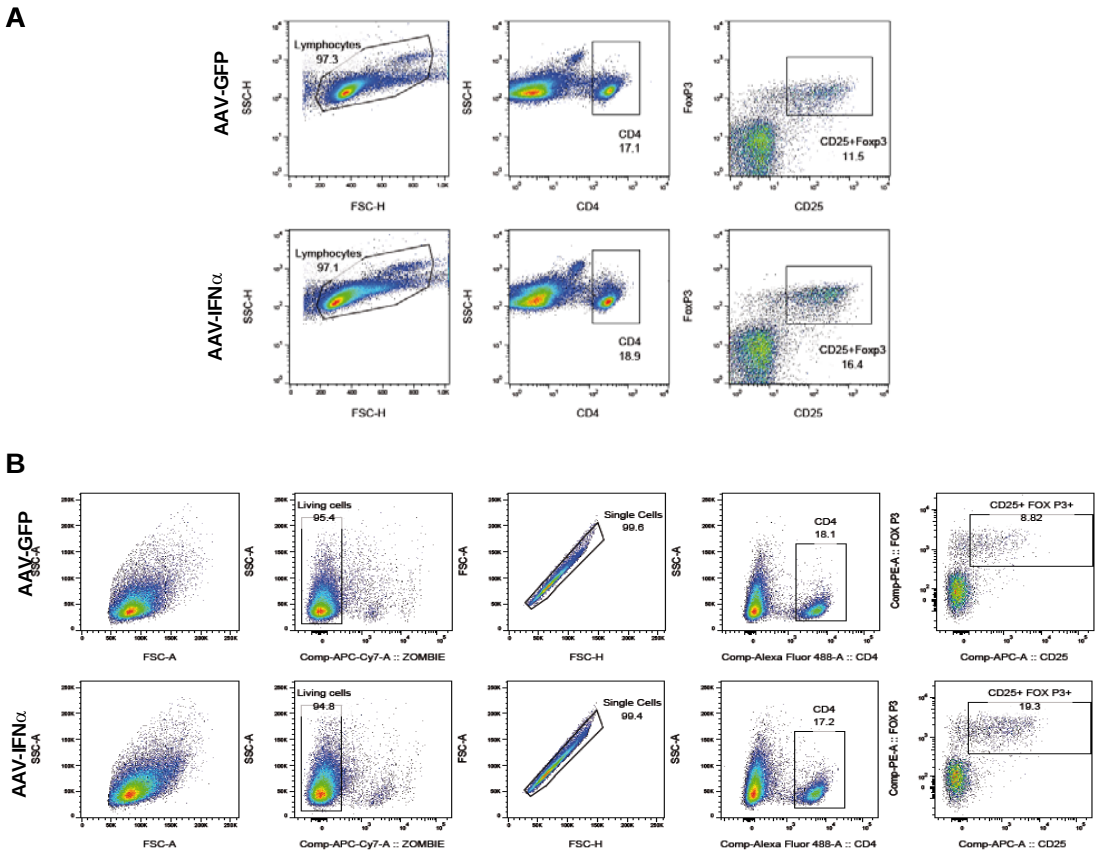

Figure S2: Gating strategy for regulatory T cell analysis. Representative analysis of regulatory T cells (CD4+CD25+FoxP3+) in spleens from mice treated with AAV-GFP (1x1010 vg) or IFN-α (1x1010 vg) four days after being mock-immunized **(A)** or immunized with MOG **(B)**

Sustained low dose IFN-α decreases EAE-immune mediators

Histological analysis was carried out to correlate symptoms with the inflammatory and demyelinating course of the disease, as occurs in MS. Control mice with high EAE scores had lymphocyte infiltrates in the peripheral regions of the spinal cord in the lumbar region, as indicated by the presence of several nuclei within the white matter. Treatment with sustained low-dose AAV-IFN-α decreased the immune cell infiltration (Figure 5A and 5B). A demyelinating pattern, defined by a less intense staining of the

white matter in the periphery, was also observed in the same regions of the spinal cord where the infiltrates were found. As expected, the reduced infiltration achieved by AAV-IFN-α inversely correlated with demyelination and this parameter returned to baseline levels in mice that received the AAV-IFN-α (Figure 5C and 5D).

To further characterize the immune cells infiltrating the spinal cord, we performed real-time PCR of several immune-related transcripts 14 days after MOG immunization. All the immune-related markers analyzed (CD4, FoxP3, IFN-γ, IL-17A and F4/80) were upregulated in the spinal cord of mice treated with AAV-GFP while the levels of these markers were significantly reduced in mice treated with AAV-IFN-α (Figure 5E).

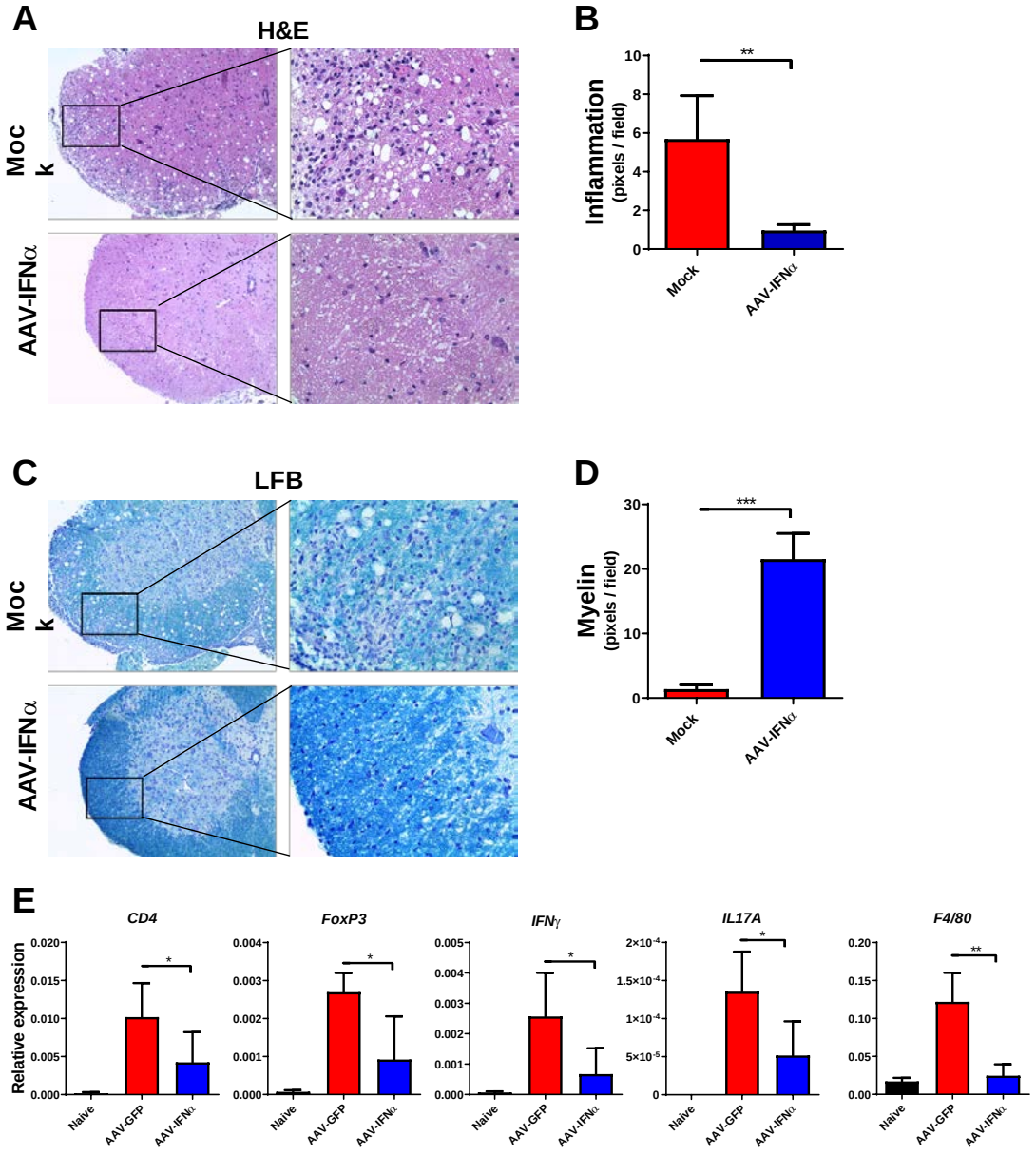

Figure 5. Sustained low-dose IFN-α decreases EAE-immune mediators. AAVs encoding GFP or IFN-α ($1x10^{10}$ vg) were administered to C57BL/6 mice (n = 12 per group) four days after MOG immunization. At day 21, histological and mRNA analyses of the spinal cord were performed. **(A)** A representative H&E staining is shown. **(B)** Inflammation was quantified by measuring pixel density. **(C)** A representative image of luxol fast blue (LFB) staining is shown. **(D)** Myelin was quantified by measuring image intensity. **(E)** Quantitative real-time PCR analysis of mRNA levels of different immune-related genes from spinal cord samples. Data are expressed as mean ± SD. (t-test for B

and E; One-way ANOVA followed by Bonferroni post-test for E. $**p < 0.01$, $***p < 0.001$).

This unspecific anti-inflammatory activity was accompanied by an antigen-specific dampened immune response. Splenocytes from mice treated with AAV-IFN-α re-stimulated with MOG peptide *in vitro* showed an up-regulated mRNA expression levels of immunosuppressive molecules such as interleukin 10 (IL-10), indoleamine-2,5-dioxygenase (IDO) and programmed death 1 (PD-1) (Figure 6A). In line with the immunosuppressive program activated by re-stimulation with the MOG peptide, splenocytes showed both reduced proliferation (Figure 6B) and release of IL-17A and IFN-γ cytokines (Figure 6C and Supplemental Fig. 3). Moreover, reduced intracellular IL-17A and IFN-γ cytokine levels were also detected in $CD4^+$ cells (Figure 6D). To demonstrate the reduced encephalitogenic capacity of MOG-specific spleen T cells from AAV-IFN-α-treated mice, we expanded them in the presence of MOG_{35-55} peptide, recombinant mouse interleukin 12 and anti-mouse IFNγ antibody for further infusion into WT mice. The administration of $10x10^6$ cells to WT C57BL/6 mice induced clinical symptoms that peaked 10 days after cell infusion. In contrast, mice that received spleen cells from mice treated with AAV-IFN-α only exhibit mild clinical symptoms and no weight loss.

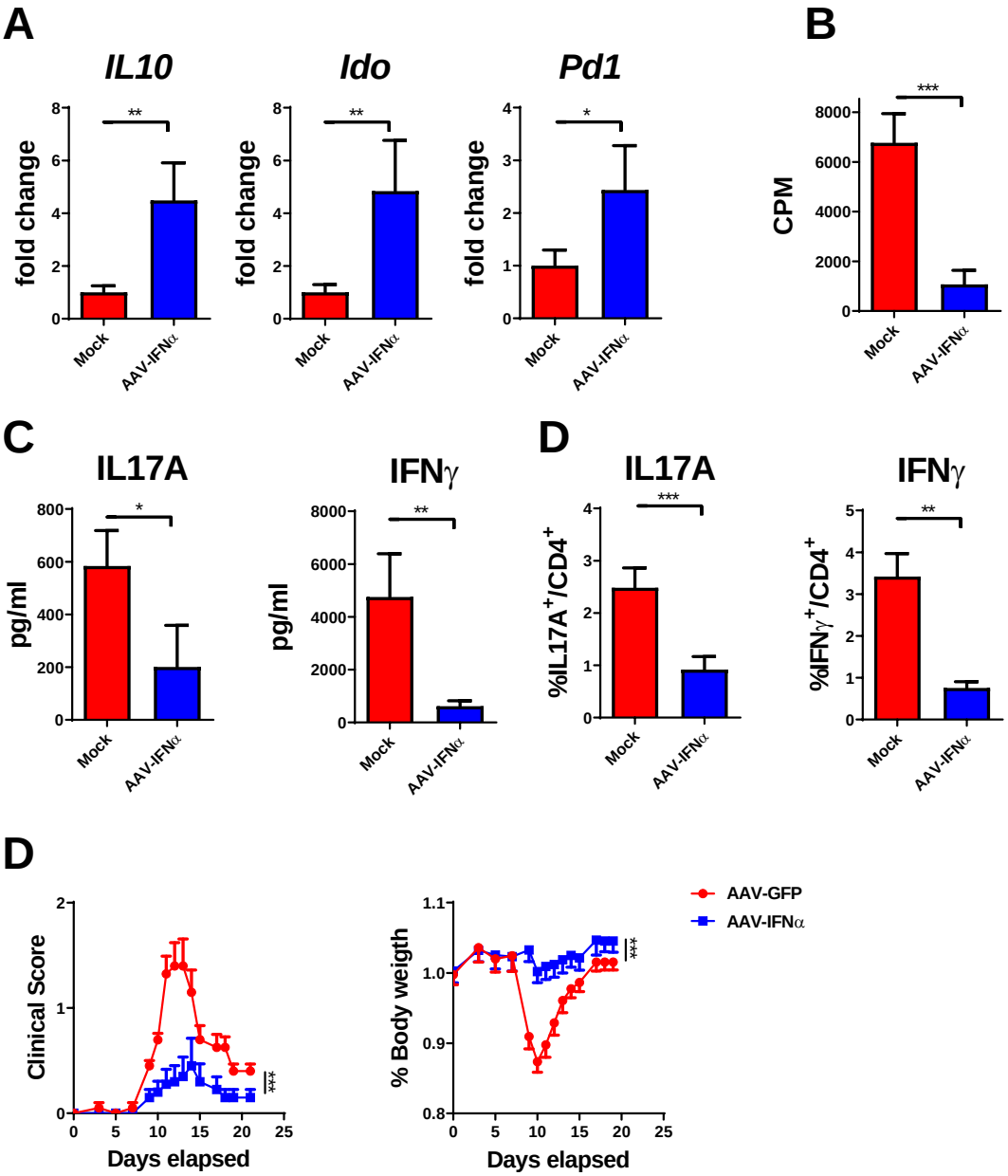

Figure 6. Sustained low-dose IFN-α increases anti-inflammatory markers and reduces proliferation and IL-17A/IFN-γ production in response to MOG restimulation. C57BL/6 mice were immunized and treated with AAV-IFN-α four days immunization. At day 21 mice were sacrificed, and splenocytes isolated and stimulated with MOG peptide *in vitro*. **(A)** mRNA levels of *IL10*, *Ido* and *Pd1* were determined by quantitative real-time PCR. **(B)** A [^{3}H]-thymidine incorporation assay was performed in

splenocytes incubated with the MOG peptide (50µg/ml) for 72 h at 37 °C**. (C)** IL-17A and IFN-γ levels were quantified in the supernatant by ELISA **(D)** or intracellular by flow cytometry in splenocytes incubated with MOG peptide (50µg/ml) for 72 h at 37 °C. Data are expressed as mean ± SD. (t-test. *$p < 0.05$, **$p < 0.01$, ***$p < 0.001$). Splenocytes incubated for three days in the presence of MOG, plus recombinant mouse IL-12 and anti-mouse IFN-γ antibody were inoculated to C57BL/6 mice. Clinical score **(E)** and body weight **(F)** were determined. Data are expressed as mean ± SD. (t-test. *$p < 0.05$, **$p < 0.01$, ***$p < 0.001$). Data are expressed as mean ± SEM and analyzed by extra sum-of-squares F test, ***$p < 0.001$.

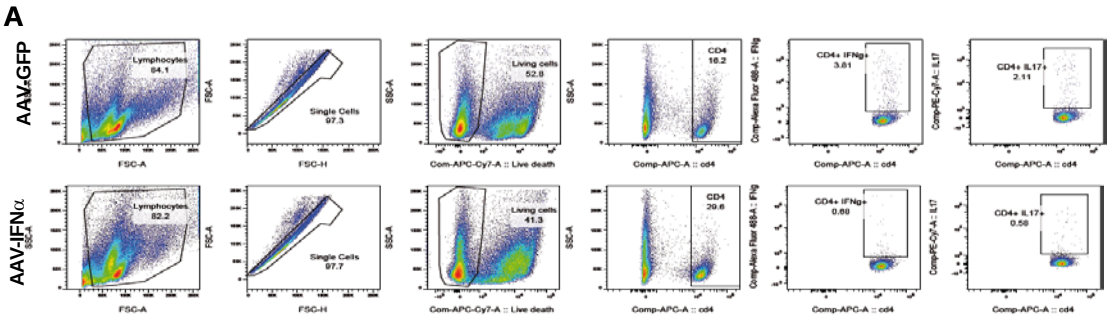

Figure S3: Gating strategy for the IL-17A/IFN-γ production analysis. Representative analysis of IL-17A and IFN-γ levels in splenocytes incubated with MOG peptide (50µg/ml) for 72 h at 37 °C from mice treated with mock or IFN-α (1x1010 vg) four days after being immunized with MOG.

Discussion

Cytokines are soluble mediators of the immune response. Tightly controlled release and short half-life in circulation are common characteristics that ensure timely crosstalk among immune cells. Mimicking these biologic properties of cytokines is a major hurdle for the clinical use of recombinant cytokines. The use of recombinant proteins as drugs requires administration of high doses to reach relevant concentrations at the target site. However, *i.m.* or *s.c.* injections produce peaks and valleys pharmacokinetic profile. Thus, plasma concentrations fluctuate often falling outside the therapeutic range with long periods of supra- and infra-therapeutic plasma concentrations. These pharmaceutical issues are exemplified by the clinical use of type I interferons for the treatment of relapsing-remitting MS and have led to the approval of five different IFN-β drugs. Although compelling evidence is lacking, frequent administration of IFN-β has a beneficial effect on annualized relapse rates (39). An alternative to this approach that is also available for patients with MS is pegylated IFN-β. The binding of 20 kDa polyethylene glycol to IFN-β prolonged its half-life in circulation at the expense of reducing the specific activity. A single dose every two or four weeks of this chemically modified IFN-β is as efficient and safe as other IFN-drugs that required several administrations per week (40). In this study, we sought to determine the viability of sustained exposure to the IFN-α1 cytokine using the EAE mouse model. It has been shown previously that hydrodynamic administration of a plasmid encoding IFN-β was able to reduce the symptoms for one month (41). The use of an adeno-associated virus allowed us to take this concept to the extreme. After administration of hepatotropic AAV-8, transduced hepatocytes continuously release the protein encoded by the gene of interest. Plasma levels reach a stable concentration within the first two weeks post-administration, and this plasma concentration is maintained throughout the lifespan of

mice. In our hands, the administration of AAV-IFN-α exerted a potent therapeutic effect that allowed titrating down the virus to a dose of 1x 10^{10} vg per mouse. We have previously reported that this dose does not exert an antitumor effect against colon cancer cells implanted in the liver (12) but produced detectable amounts of the cytokine in circulation. These IFN-α levels also induced the expression of IFN-stimulated genes in circulating Tregs and remodeled the immune cells in the spleen, promoting Ly6C expression on monocytes, reducing neutrophils and expanding Treg cells.

Moreover, this low dose of IFN-α decreased the immune cell infiltration and demyelination of the spinal cord, and dampened the immune response against the MOG peptide. Finally, the low doses of AAVs used in this study were safe and we did not detect hematological or neurological adverse events. Thus, this study illustrates the safety and therapeutic potential of sustained delivery of low-dose IFN-α cytokine.

The concept of low-dose cytokine has entered into clinical trials thanks to the use of low-dose IL-2 for the treatment of several autoimmune diseases such as type 1 diabetes and autoimmune hepatitis (42, 43). This study supports the putative translation of the concept of low-dose cytokines to the treatment of relapsing-remitting MS with IFN-β. However, the uncontrolled release of IFN-β/α from a gene therapy vector could lead to unacceptable severe adverse effects. The use of sophisticated inducible promoters or suicide genes could solve these problems but may have clinical development challenges. Thus, in order to translate this concept to the clinical arena, the fusion of IFN-α to apolipoprotein A-1 could be a promising alternative. Higher doses of AAVs coding for IFN-α/ApoA1 fusion protein were required to achieve a therapeutic effect when compared with the AAV-IFN-α. This tempered activity would be favorable when using other delivery strategies such as modified mRNA (44, 45) or *s.c.* administration of the recombinant fusion protein (46). The deleterious peaks and valleys

pharmacokinetic profile could be minimized by the increased half-life in circulation and consequently reduce the cytotoxic activity of the fusion protein (38).

The sustained release of low doses of IFN-α leads to a significant increase in Treg cells defined as $Foxp3^+$ cells within the $CD4^+$ population. The role of IFN-α on Treg cell development remains controversial. Early reports showed that both exogenous and endogenous type I IFNs promoted effector $CD4^+$ T lymphocytes with low or negative FoxP3 expression and reduced the percentage of $CD4^+$ cells that expressed high levels of FoxP3 (47). However, experiments using mixed bone marrow chimeras between wild-type and IFN-α/βR knockout (KO) mice highlighted a role for type I IFNs in the development of Treg cells (48). It is also known that treatment with IFN-β can induce $CD4^+CD25^+Foxp3^+$ Treg cells in some patients with MS (49). Moreover, IFN-α has been previously shown to disarm Treg suppressive function (without affecting FoxP3 expression) by downregulation intracellular cAMP level (50). Thus, the long-term functional outcome of the two opposing effects (expansion and deactivation) of IFN-α on Treg cells remains to be determined.

In conclusion, sustained low-dose delivery of IFN-α1 or IFN-α1 fused to apolipoprotein A-1 improved symptoms of the EAE by immune cell remodeling. Thus, feasible clinical strategies to translate the concept of low-dose immunotherapy to relapsing-remitting MS may improve the management of the disease.

Acknowledgments

The authors acknowledge Paul Miller for English editing. This work was supported by grant from Fondo de Investigación Sanitaria (PI16/00668) to PB, and grants from Worldwide Cancer Research (14-1275), Fundació La Marató TV3 (201319-30), and Spanish Ministerio de Economía y Competitividad (SAF2016-80535-R) -co-financed by European Development Regional Fund "A way to achieve Europe" ERDF- to FL. PB and FA are supported from Instituto de Salud Carlos III by Miguel Servet II (CPII15/00004) contract and Sara Borrell Program (CD15/00016). IS and EC are recipients of fellowships from Fundação para a Ciência e a Tecnologia (SFRH/ BD/75738/2011), and European Community Seventh Framework Program (BIOTRACK, FP7/2007/2013; 229673), respectively.

Chapter 2 : “Statins act as transient type I interferon inhibitors to enhance the antitumor activity of Modified Vaccinia Ankara”

Title

Statins act as transient type I interferon inhibitors to enhance the antitumor activity of Modified Vaccinia Ankara

Authors

Shirley Tenesaca[1,2], Marcos Vasquez[1,2], Maite Alvarez[1,2], Itziar Otano[1,2], Myriam Fernandez-Sendin[1,2], Claudia Augusta Di Trani[1,2], Nuria Ardaiz[1,2], Celia Gomar[1,2], José Medina-Echerverz[3], Ignacio Melero[1,2,4,5], Pedro Berraondo[1,2,4,*]

Affiliations

[1]Program of Immunology and Immunotherapy, Cima Universidad de Navarra, Pamplona, Spain.

[2]Navarra Institute for Health Research (IDISNA), Pamplona, Spain.

[3]Bavarian Nordic GmbH, Martinsried, Germany.

[4]Centro de Investigación Biomédica en Red de Cáncer (CIBERONC), Spain.

[5]Department of Oncology, Clínica Universidad de Navarra, Pamplona, Spain

Abstract

Modified vaccinia virus Ankara (MVAs) are genetically engineered non-replicating viral vectors. Intratumoral administration of MVAs induces a cGAS-mediated type I interferon response and the production of high levels of the transgenes encoded by the engineered viral genome such as tumor antigens to generate cancer vaccines. Although type I interferons are essential for establishing CD8-mediated antitumor responses, this cytokine family also gives rise to immunosuppressive mechanisms that might limit the antitumor efficacy of MVAs. In this work, we identified commonly prescribed statins as potent IFN-α pharmacological inhibitors due to their ability to reduce the membrane expression of IFN-α/β receptor 1 and to reduce clathrin-mediated endocytosis. Indeed, Simvastatin and atorvastatin efficiently inhibited for 8 hours the transcriptomic response to IFN-α. In vivo, intraperitoneal or intramuscular administration of simvastatin enhanced the antitumor activity of MVA encoding ovalbumin against B16 ovalbumin-expressing tumors. The synergistic antitumor effects depend critically on $CD8^+$ cells and whereas they were markedly improved by depletion of $CD4^+$ or NK lymphocytes. Both MVA-OVA alone or combined with simvastatin augmented B cells, $CD4^+$ lymphocytes, $CD8^+$ lymphocytes, and tumor-specific $CD8^+$ in the tumor-draining lymph nodes compared to MVA alone. The treatment combination increased the numbers of these immune cell populations in the tumor microenvironment. In conclusion, blockade of IFN-α functions by simvastatin enhances lymphocyte infiltration and the antitumor activity of MVAs prompting a feasible drug repurposing.

Introduction

Decades of preclinical research in cancer virotherapy have now led to numerous clinical trials and the first regulatory approval of an armed virus for the treatment of melanoma. Talimogene Laherparepvec (T-VEC) is an oncolytic herpes virus genetically modified to encode GM-CSF. In 2015, this virus was approved by the FDA for the treatment of unresectable advanced melanoma (51). Herpes virus and other oncolytic viruses such as Newcastle disease virus, reovirus, or adenovirus are engineered to replicate selectively in malignant cells. The dying tumor cells show the hallmarks of immunogenic cell death that trigger the activation of the immune system not only to the viral antigens but also to tumor-associated antigens. Poxvirus such as these derived from strains of vaccinia virus are in clinical development. The immunogenicity of the virus-induced tumor cell death is enhanced in some instances by the expression of immunostimulatory proteins encoded by the recombinant viral genome such as GM-CSF in the case of T-VEC (52).

In other cases, viruses are used merely for their capacity to trigger a potent immune response and non-replicative viruses are used as immunotherapies. This is the case of modified vaccinia virus Ankara (MVA). MVA was developed by Professor Anton Mayr after 516 passages of the Chorioallantois vaccine Ankara strain of the vaccinia virus on primary chicken embryo fibroblasts. This process gave rise to a loss of 15 % of the parental genome. The genomic deletions affect multiple virulence factors rendering MVA defective for replication in human cells or immune-suppressed mice (53). The immunogenicity of MVA relies on the activation of the STING pathway. cGAS detects cytosolic dsDNA and, through the activation of an intracellular signaling cascade that involves STING, triggers the release of type I interferons. The IFN release is required

for the activation of specialized cross-presenting dendritic cells (cDC1s) (54). Bavarian Nordic has developed MVA-based vaccines against several infectious diseases and is also exploring the potential of MVA in cancer immunotherapy. PROSTVAC, an antitumor vaccine that includes an MVA, was evaluated in a phase III clinical trial for the treatment of prostate cancer. PROSTVAC combines two poxviral-based vectors in a prime and boost strategy. The first virus is a recombinant vaccinia virus, and the second a recombinant fowlpox virus. Both viruses encode prostate-specific antigen as a tumor-associated antigen and as immunomodulatory proteins encode CD80, leukocyte function-associated antigen-3, and intercellular adhesion molecule-1. The phase III clinical trial did not meet the primary endpoint of overall survival (55) suggesting that further improvements in vaccinia –based vaccines are needed.

To enhance the efficacy of virotherapy, we have focused on the transient blockade of type I interferon signaling. Interferon-beta and the various subtypes of interferon-alpha are released after the activation of pathogen- or damage-associated molecular pattern receptors. The most potent inductors of type I IFN are the ligands of TLR-3, the ligands of cytosolic RNA receptors such as RIG-I and MDA-5, or the ligands of cytosolic DNA receptors such as cGAS (45, 56, 57). Type I IFNs interact with the interferon-alpha/beta receptor, leading to the activation of the JAK-STAT, MAPK, PI3K and Akt pathways. The activation of these pathways exerts potent antitumor effects. The mechanism involves a direct effect on malignant cell proliferation, the blockade of angiogenesis, and the activation of T lymphocytes and NK cells (58, 59). However, type I IFNs also induce the upregulation or downregulation of hundreds of genes that lead to an antiviral program in the cells (60). This antiviral cellular programming establishes a viral refractory state that involves suppression of viral replication and of viral gene transcription. Transient blockade of the type I IFN signaling might allow efficient viral

replication or transgene expression while the IFN receptor is functionally silenced, but when it is restored could trigger strong antitumor IFN-mediated activity, once maximum transgene expression has been achieved. This transient inhibition concept has been used to enhance the antitumor activity of oncolytic viruses. Ruxolitinib, a JAK inhibitor, was used to increase the replication of Measles virus (61), herpes simplex virus (62) and vesicular stomatitis virus encoding IFN-β (63). Other pathways targeted to block type I IFN production have been the mammalian target of rapamycin complex 1 (mTORC1) (64) and the NFκB (65). The specific drug VSe1-28 has been developed with the purpose of blocking type I IFN activity and enhancing viral replication (66).

Statins are widely used drugs for the treatment of hypercholesterolemia, but they are also potent anti-inflammatory molecules. The primary mechanism of action involves the inhibition of the 3-hydroxy-3-methylglutaryl coenzyme A (HMG-CoA) reductase. The blockade of this enzyme decreases cholesterol synthesis and circulating LDL cholesterol levels but also inhibits protein isoprenylation and therefore alters several signaling proteins such as RAS, RAC, and Rho (67). Recently, it has been reported that lipophilic statins such as simvastatin block the geranylgeranylation of Rab5 in dendritic cells and enhance the efficacy of antitumor vaccines (68). Here, we find that both the lipophilic statin simvastatin and the polar statin atorvastatin are potent inhibitors of the interferon-alpha signaling due to the blockade of the clathrin-mediated endocytic pathway. *In vivo* simvastatin is a potent enhancer of the antitumor activity of MVA since simvastatin promotes the infiltration of effector immune cells into the tumor microenvironment.

Materials and methods

Cell lines and culture media

The L929 murine fibroblast cell line was purchased from ATCC and was cultured in medium consisting of DMEM (Gibco, Karlsruhe, Germany) supplemented with 2 mM glutamine (Sigma-Aldrich, Taufkirchen, Germany), 100 IU penicillin, 100 µg/ml streptomycin (Gibco), and 10% (v/v) fetal bovine serum (FBS; Gibco) in a humidified incubator at 37°C and 5% CO_2. B16-OVA cells were provided by Dr. Lieping Chen (Yale University, New Haven, CT) and were cultured in medium RPMI 1640 (Gibco) supplemented like DMEM, but with addition of 50 µM β-mercaptoethanol (Sigma-Aldrich) and geneticin G418 400 µg/ml (InvivoGen, San Diego, CA).

Reagents

Modified vaccinia Ankara-Bavarian Nordic expressing OVA (MVA-mBNbc 126 36A18-A) was provided by Bavarian Nordic A/S (Kvistgaard, Denmark) as a liquid-frozen product (0.5 mL) with a nominal titer of 4.22×10^{9} $TCID_{50}$ /ml. Mouse IFN Alpha 1 protein was obtained from PBL Assay Science (Catalog No. 12105-1; Piscataway, NJ). Simvastatin (PHR1438-1G) and Atorvastatin Calcium (PHR1422-1G) were purchased from Sigma-Aldrich and were reconstituted in methanol. BSA-FITC was acquired from Sigma Chemical Co. (St. Louis, MO). Trypan blue was obtained from Sigma-Aldrich.

Flow cytometry analysis

Flow cytometry analysis was performed using a FACS Canto II flow cytometer (BD Biosciences, San Diego, CA) and a CytoFLEX LX apparatus (Beckman Coulter, Miami, FL). The following antibodies were used and acquired from BioLegend (San Diego, CA): PE anti-mouse IFNAR-1 (MAR1-5A3), Zombie NIR, Brilliant Violet 650™ anti-mouse CD19 (6D5), Brilliant Violet 510™ anti-mouse CD45 (30-F11), Brilliant Violet 605™ anti-mouse TCR β chain (H57-597), 7-AAD Viability Staining Solution. These were acquired from BD Biosciences: BUV395 Rat Anti-Mouse CD8a (53-6.7), BUV496 Rat Anti-Mouse (GK1.5), Purified Rat Anti-Mouse CD16/CD32 antibody (Mouse BD Fc Block). PE-conjugated H-2K^{b}/OVA $_{257–264}$ complex was obtained from MBL Co., Ltd. (Nagoya, Japan)

RNA isolation and quantification of mRNA

RNA was isolated from the studied cell lines and tissues using the Maxwell® 16 Total RNA Purification Kit (Promega, Madison, WI), quantified in a NanoDrop spectrophotometer (Thermo Scientific, Wilmington, DE), and retrotranscribed (300 ng) to cDNA with Moloney murine leukemia virus (M-MLV) reverse transcriptase from Promega, according to the manufacturer's instructions.

Quantitative real-time PCR was performed with iQ SYBR Green Supermix (Bio-Rad, Hercules, CA) using specific primers for each gene; they were purchased from Invitrogen (Thermo-FisherScientific, USA). RLP0 5'-aacatctccccttctcctt-3' 5'-gaaggccttgacctttcag-3', USP18 sense 5'-ccaaaccttgaccattcacc-3' USP18as 5'-atgaccaaagtcagcccatcc-3', ISG15sense 5'-gattgcccagaagattggtg-3' ISG15as 5'-

tctgcgtcagaaagacctca-3', 2,5 OAS sense 5'-actgtctgaagcagattgcg-3' 2,5 OAS as 5'-tggaactgttggaagcagtc-3'. As RLP0 levels remained constant across different experimental conditions, this parameter was used to standardize gene expression. The amount of each transcript was expressed by the formula 2ΔCt, with ct being the point at which the fluorescence rises significantly above background levels.

Expression of IFNR1 and endocytosis evaluation

First, L929 cells (3 x10^4 /well) were seeded in 96-well plates in triplicate in DMEM 10% FBS culture media. After 24 hours, they were washed with PBS and treated for 3 hours with decreasing dilutions of the studied drugs or vehicle on 150µl of DMEM without fetal bovine serum. Simvastatin and atorvastatin dilutions were made from 600 µM until 6.5 µM from a 10 mM stock. Then, cells were detached with 50 µl of trypsin-EDTA (Gibco), washed and stained for IFNAR-1 detection with 50 µl of a cocktail of PE anti-mouse IFNAR-1 (1:200), Zombie NIR (1:1000) and BD Fc Block (1:200) for 20 minutes at 4º C. For the BSA-FITC endocytosis assay, cells were treated with atorvastatin (300 µM), simvastatin (37.5 µM) or vehicle methanol (7.5 µl) under the same conditions described above, but after 3 hours of incubation they were washed with PBS and were incubated for 3 hours with DMEM 10% FBS. Then, the culture medium was removed and replaced by 150 µl of DMEM with BSA FITC (100 µg/ml), and cells were incubated for 1 hour for BSA endocytosis. After the last treatment, cells were detached, washed and stained with 7-AAD (1:75) in 50 µl of PBS for 15 minutes. Finally, they were resuspended in 200µl of PBS with trypan blue (250 µl/ml) for cytometric analysis.

IFN-α signaling evaluation

L929 cells (8 x10^4 /well) were seeded in 24-well plates in triplicate in DMEM 10% FBS culture media. After 24 hours they were washed with PBS and treated for 3 hours with atorvastatin (300 µM), simvastatin (37.5 µM) or vehicle (MeOH, 7.5 µl) in 250µl of DMEM without fetal bovine serum. Afterward, cells were washed with PBS and were kept for 0, 3, 6 and 9 hours with DMEM 10% FBS. Next, cells were stimulated with IFN Alpha 1 protein (100 units/ml) for 3 hours in 250 µl of DMEM 10% FBS. Lastly, the culture medium was removed, and the cells collected for RNA extraction.

Western blotting

L929 cells (1 x10^6 /well) were seeded in 6-well plates using DMEM 10% FBS and incubated for 24 h. Atorvastatin (300 µM), Simvastatin (37.5 µM) or vehicle (MeOH) treatment was performed for 3 h using DMEM without fetal bovine serum. Then, the supernatant was eliminated and IFNa (3000 units/ml) were added for 30 minutes. Finally, phosphorylation of STAT-1 was analyzed by Western blot using the appropriate antibodies.

Animal experimentation

In vivo experiments were performed with 6 to 8 week-old female C57BL/6 mice purchased from Harlan Laboratories (Barcelona, Spain). The mice were kept under

specific pathogen-free conditions. The experimental design was approved by the Ethics Committee for Animal Testing of the University of Navarra.

Antitumor activity assay

2.5 x 10^5 B16OVA cells were inoculated subcutaneously on the right hind flank of C57BL/6 mice; the mice were randomized at day 7 and treated at days 7 and 14 after implantation. 20 µg of simvastatin per mouse were injected intra-peritoneally or intra-muscularly in 100 µl of PBS. After two hours, the MVA vaccine was administered subcutaneously next to the tumor area at a concentration of $5x10^7$ $TCID_{50}$ per mouse in 100 µl of PBS. In the case of intramuscular administration, the MVA vaccine was administered simultaneously. Tumor sizes were measured twice weekly using electronic calipers and mice were euthanized when tumors reached 17 mm on the longest axis.

Lymphocyte population depletions

The tumor model and treatment regimen were as in the antitumor activity assay but mice were depleted of $CD4^+$ T cells using anti-mouse CD4 monoclonal antibody (clone GK1.5, BioXCell, L'Aigle, France), $CD8^+$ T cells using anti-CD8β (clone H35-17.2, in house), NK cells using anti-mouse NK1.1 (clone PK136, BioXCell). 200 µg of each antibody per mouse were administered intra-peritoneally one day before first therapeutic treatment administration and on days 2, 6, 9, and 13 after it.

Immune cell analysis

The tumor model was performed as in the antitumor activity assay, but, in this case, mice received a single dose of treatment. Tumor tissues, lymph nodes, and spleens were collected on day five after treatment and were processed for cytometric analysis as described in (69).

Analysis of interferon-stimulated genes in tumor tissues

The tumor model was performed as in the antitumor activity assay, but, in this case, mice received a single dose of the treatment. Tumor tissues were collected in RNA homogenization buffer at 4 hours after treatment and were stored at - 80°C until they were processed.

Statistical analysis

GraphPad Prism version 8.2.1 software (GraphPad Software, Inc., San Diego, CA) was used for statistical analysis. Data were analyzed by one-way ANOVA followed by Dunnett's multiple comparisons test. P values <0.05 were considered to be statistically significant.

Results

Screening of potential pharmacological type I IFN inhibitors

We conducted a screening of clinically approved drugs to find novel inhibitors of the type I interferons. The selection was based on two assays. First, we analyzed the reduction of the membrane levels of the interferon-alpha/beta receptor 1. The second assay focused on the interference with the endocytosis pathway. These assays were based on the differential outcome of type I interferon signaling depending on the cellular IFNR density and on the fact that clathrin-dependent endocytosis of activated IFNR complex is required for type I interferon signaling (70, 71). Several compounds successfully reduced both IFNR1 levels and bovine serum albumin endocytosis. Among these, we focused our attention on two statins, simvastatin, and atorvastatin. Both compounds reduced the membrane levels of IFNR1 in a dose-dependent manner. The maximum reduction was around 40% of baseline levels. The maximum effect was achieved at 37.5 μM for simvastatin and 300 μM for atorvastatin (Figure 1A to D). Simvastatin was not toxic for the L929 cells at the dose range tested, and the level of viable cells analyzed by 7AAD incorporation was higher than 95% in all tested concentrations. Atorvastatin was slightly more toxic in culture, and at the dose of 300 μM, only 69% of cells remained alive. Dead cells were excluded from the IFNR1 expression analysis. Based on these assays we selected the effective dose of simvastatin and atorvastatin. Using these doses, we analyzed the internalization of bovine serum albumin (BSA) labeled with fluorescein 5(6)-isothiocyanate (FITC). We have previously shown that BSA internalization is inhibited at 4ºC and by treatment with chlorpromazine, as expected for a clathrin-mediated-process (72). Both compounds significantly inhibited fluorescent BSA uptake (Figure 1 E and F).

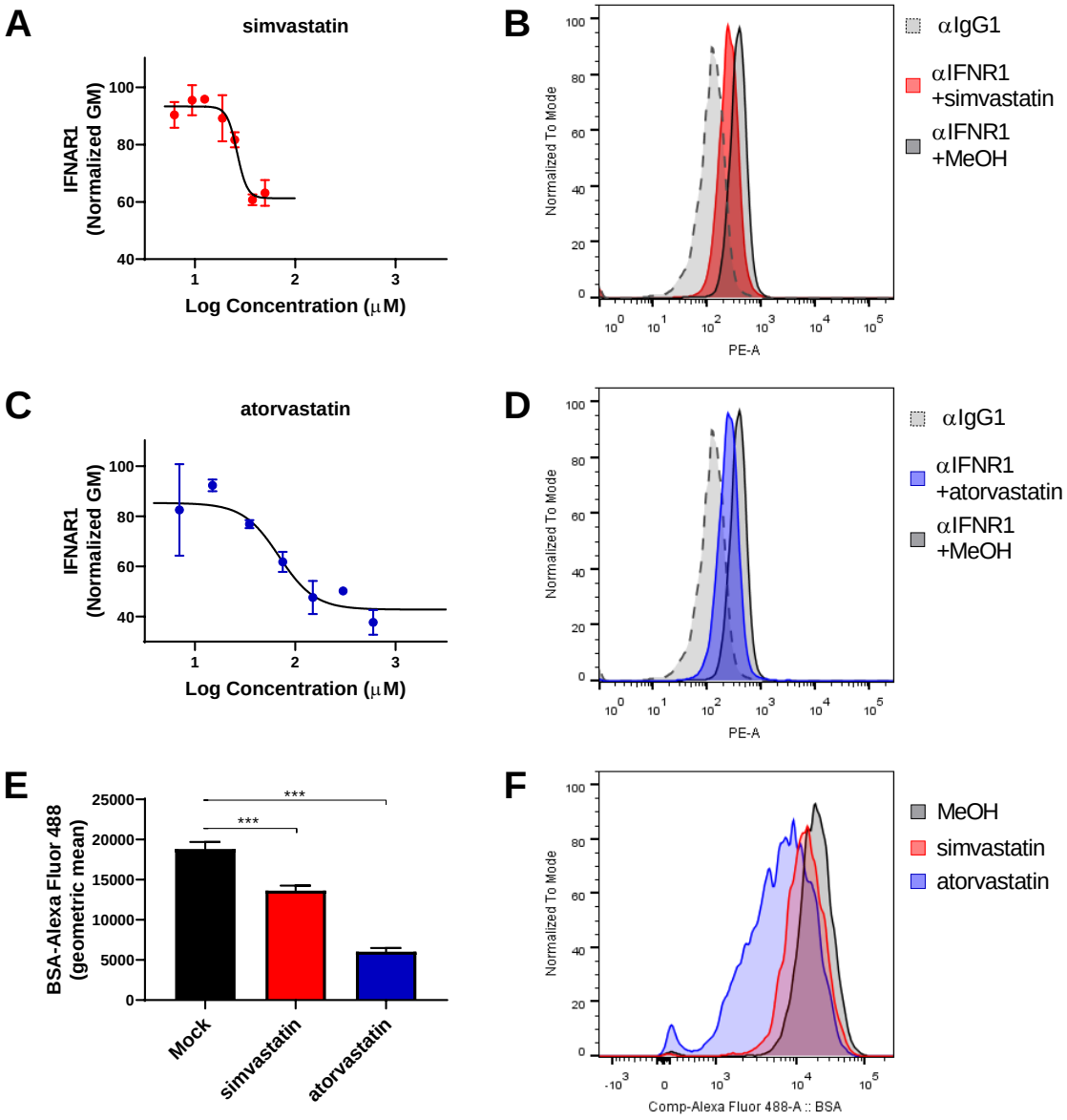

Figure 1. Simvastatin and atorvastatin reduce the expression of IFNR1 and endocytosis. (A) L929 cells were incubated with different concentrations (from 600µM until 6.5 µM) of Simvastatin for 3 hours, and levels of IFNR1 on the cell membrane were quantified by flow cytometry. **(B)** Representative histogram of mock-treated cells without αIFNR1 staining (black dashed line), simvastatin treated cells stained with αIFNR1-PE (red line) and mock-treated cells stained with αIFNR1-PE (black line). **(C)** As in A but for compound atorvastatin. **(D)** Representative histogram of mock-treated cells without αIFNR1 staining (black dashed line), simvastatin treated cells stained with αIFNR1-PE (blue line)

and mock-treated cells stained with αIFNR1-PE (black line). **(E)** L929 cells were incubated with 37.5 μM simvastatin or 300 μM atorvastatin for 3 hours, and BSA-FITC internalization was quantified by flow cytometry. One-way ANOVA followed by Dunnett's post-test. *** $p < 0.001$. **(F)** Representative histogram of simvastatin treated cells (red line), atorvastatin treated cells (blue line) and mock-treated cells (black line).

Blockade of IFN-α signaling by simvastatin and atorvastatin

Once we verified that the compounds simvastatin and atorvastatin reduced the IFNR1 membrane expression and endocytosis, we analyzed whether they were able to effectively block recombinant IFN-α-elicited signaling. The signaling cascade initiated by the binding of rIFN-α to the interferon-α/β receptor leads to the phosphorylation of STAT1 and the subsequent modulation of interferon-stimulated genes (ISGs). First we analyzed the STAT1 phosphorilation in L929 cell treated with rIFN-α alone or combined with 300 μM atorvastatin or 37.5 μM simvastatin. rIFN-α markedly increased the phosphorylation of STAT1 but this effect was totally abrogated by the co-treatemt with the statins (Figure 2A). Among these ISGs, we selected three genes as markers of the activity of rIFN-α: 2'-5'-oligoadenylate synthetase (*2,5-OAS*), interferon-stimulated gene 15 (*ISG15*) and ubiquitin-specific peptidase 18 (*USP18*). The expression of the three genes was markedly upregulated by the rIFN-α. Preincubation with simvastatin or atorvastatin 3 hours before IFN-α exposure abrogated ISGs induction (Figure 2B). The maximum inhibitory effect was observed when the IFN-α immediately followed drug withdrawal and decreased as the resting period increased. When time between the drug exposure and the IFN-α treatment was nine hours, no interaction between the drug and the IFN-α was observed (Figure 2C).

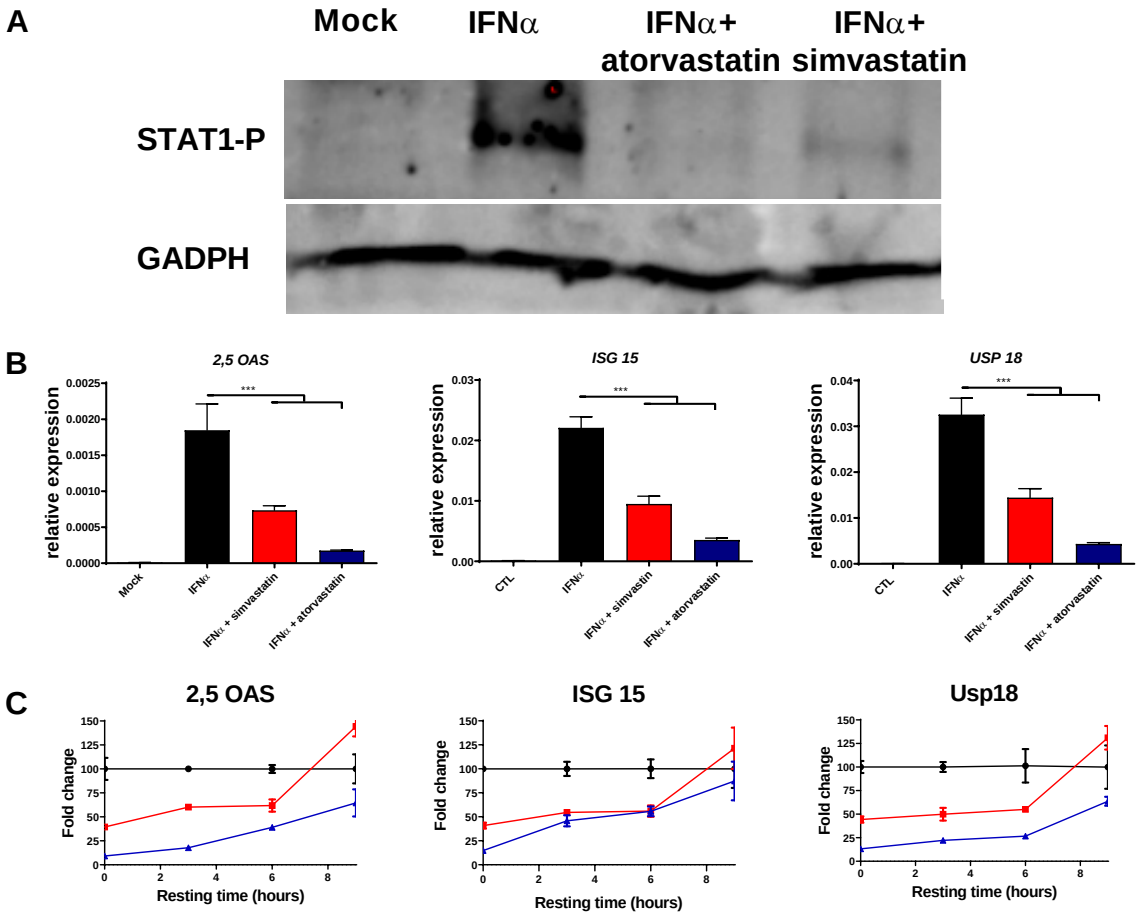

Figure 2. Simvastatin and atorvastatin reduce IFN-α induced genes.

(A) L929 cells were treated with 300 µM atorvastatin, 37.5 µM simvastatin or vehicle (MeOH) for 3 hours. Then, 3000 units/ml IFN-α were added for 30 minutes, finally phosphorylation of STAT-1 was analyzed by Western blot. **(B)** L929 cells were treated with vehicle (methanol 7.5 µl), 300 µM Atorvastatin, 37.5 µM simvastatin for 3 hours and then cells were washed. Three hours later, IFN-α (100 units/ml) was added for 3 hours, and the induction of 2'-5'-oligoadenylate synthetase (*2,5-OAS*), interferon-stimulated gene 15 (*ISG15*) and ubiquitin-specific peptidase 18 (*USP18*) was analyzed by real-time PCR. One-way ANOVA followed by Dunnett's post-test. *** p< 0.001. **(C)** L929 cells were treated with vehicle (methanol 7.5 µl), 300 µM atorvastatin, 37.5

μM simvastatin for 3 hours and then cells were washed. 0, 3, 6 and 9 hours later, IFN-α was added for 3 hours, and the induction of 2'-5'-oligoadenylate synthetase (*2,5-OAS*), interferon-stimulated gene 15 (*ISG15*) and ubiquitin-specific peptidase 18 (*USP18*) was analyzed by real-time PCR.

Simvastatin enhances the antitumor activity of MVA-OVA

Transient reduction of IFN-α/β was postulated to enhance virotherapy effects. For in vivo experiments, we selected simvastatin due to the lower doses required for the IFN-α inhibitory effect. We chose a dose based on the previous literature (68). The peritumoral injection of MVA-OVA in B16 melanoma expressing ovalbumin induced the expression of different interferon-stimulated genes, a hallmark of the release of type I IFN in response to the virus infection. Interestingly, the induction of the ISGs was inhibited by the intraperitoneal administration of simvastatin two hours before the MVA (Figure 3).

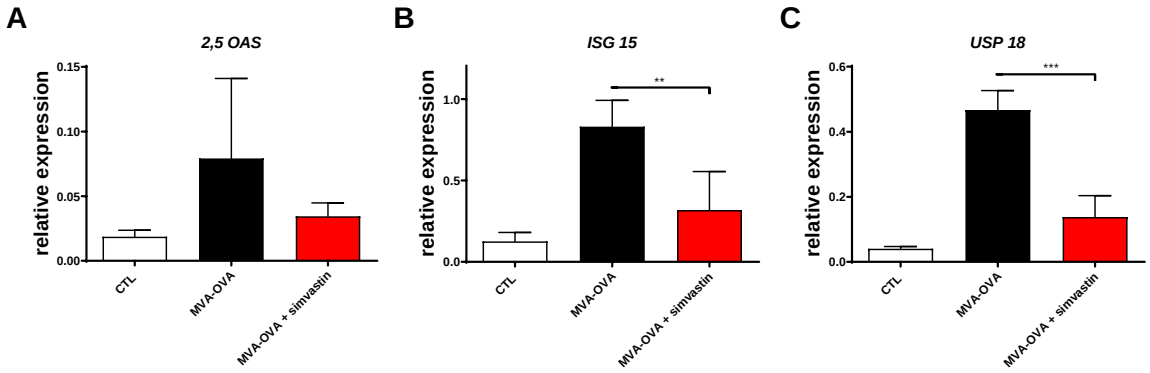

Figure 3. Simvastatin reduces interferon-stimulated genes in the tumor upon MVA infection. B16-OVA melanoma cells were injected subcutaneously. Seven days later, mice were treated intraperitoneally with vehicle or simvastatin (20 μg/mice). After 2 hours, MVA-OVA ($5x10^7$ $TCID_{50}$ per mouse) was administered subcutaneously in the

tumor area. Four hours later, mice were sacrificed and tumor mRNA quantified by real-time PCR**. (A)** 2'-5'-oligoadenylate synthetase (*2,5-OAS*) expression. **(B)** Interferon-stimulated gene 15 (*ISG15*) expression. **(C)** Ubiquitin-specific peptidase 18 (*USP18*) expression. One-way ANOVA followed by Dunnett's post-test. ** $p<0.01$ *** $p< 0.001$.

As expected, the administration of this drug alone had no impact on tumor growth (Figure 4A). The MVA-OVA was injected in the tumor and delayed tumor growth in all mice, and therefore increased survival but only completely eradicated the tumor in one mouse out of 6 (Figure 4A and B). In contrast, the administration of simvastatin intra-peritoneally or intramuscularly enhanced the percentage of cured mice at the end of the experiment. The intramuscular administration was slightly more effective and significantly increased survival as compared to the mice treated with MVA-OVA alone (Figure 4B).

MVA-OVA combined with simvastatin enhance immune infiltration in the tumor microenvironment

To evaluate the immune cells involved in the antitumor activity of the combination of MVA-OVA and simvastatin, we depleted $CD8^+$ T lymphocytes, $CD4^+$ T lymphocytes, and NK cells with monoclonal antibodies after administration of the combined treatment. The antitumor effect was dependent on $CD8^+$ T lymphocytes as depletion of these effector immune cells abrogated the antitumor effect (Figure 5A). Interestingly, both $CD4^+$ T lymphocytes and NK cells were detrimental for the antitumor effect and depletion of these immune cells led to the complete eradication of the implanted tumors in all cases (Figure 5A and B).

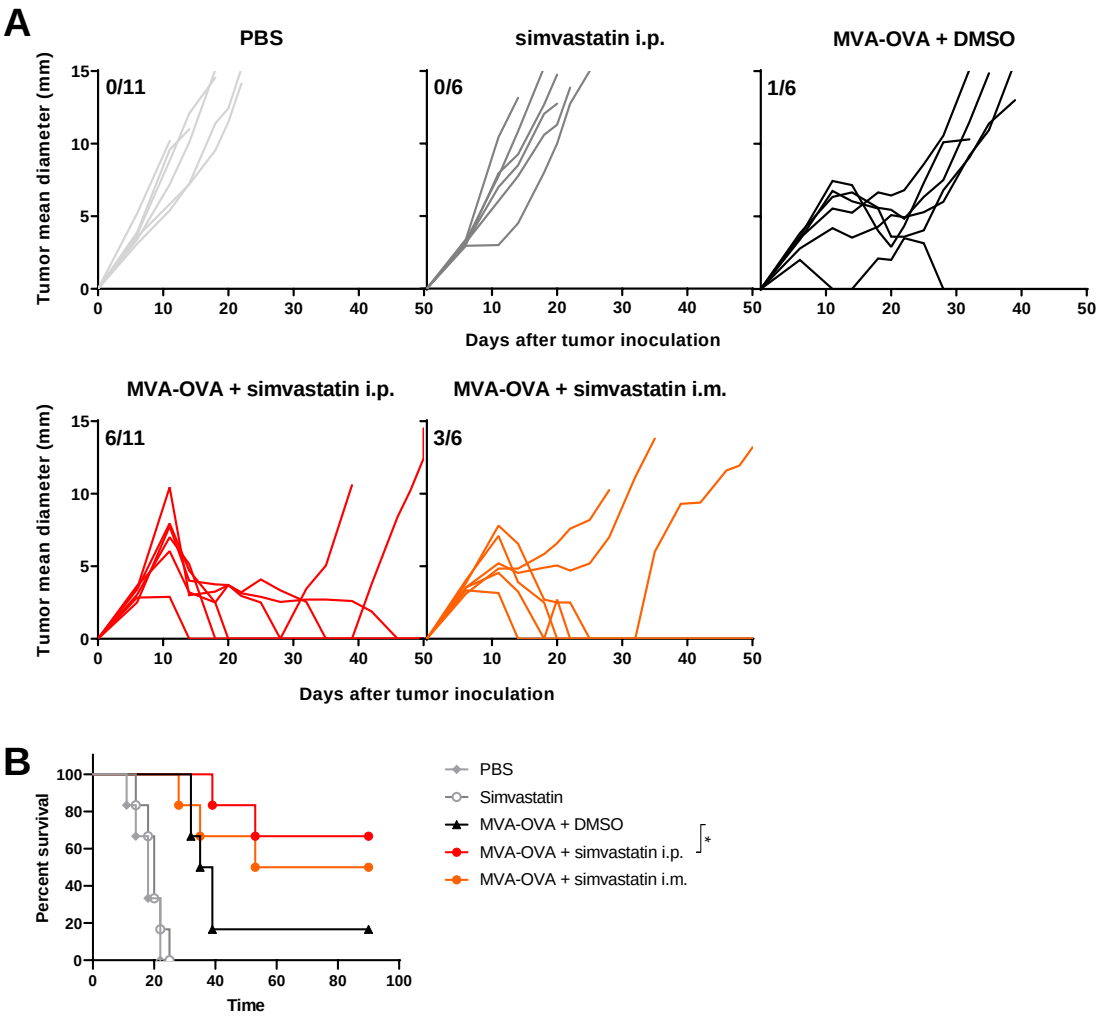

Figure 4. Simvastatin enhances the antitumor activity of MVA-OVA. B16-OVA melanoma cells were injected subcutaneously. Seven and fourteen days later, mice were treated intraperitoneally with vehicle or simvastatin (20 µg/mice). After 2 hours. MVA-OVA ($5x10^7$ $TCID_{50}$ per mouse) was administered subcutaneously in the peritumoral area. In the group treated intramuscularly with simvastatin, MVA vaccine was administered simultaneously **(A)** Individual follow-up of mean tumor diameters indicating the fraction of mice completely rejecting established tumors. **(B)** Overall survival of the indicated treatment groups. Two-sided log-rank test. * $p<0.05$.

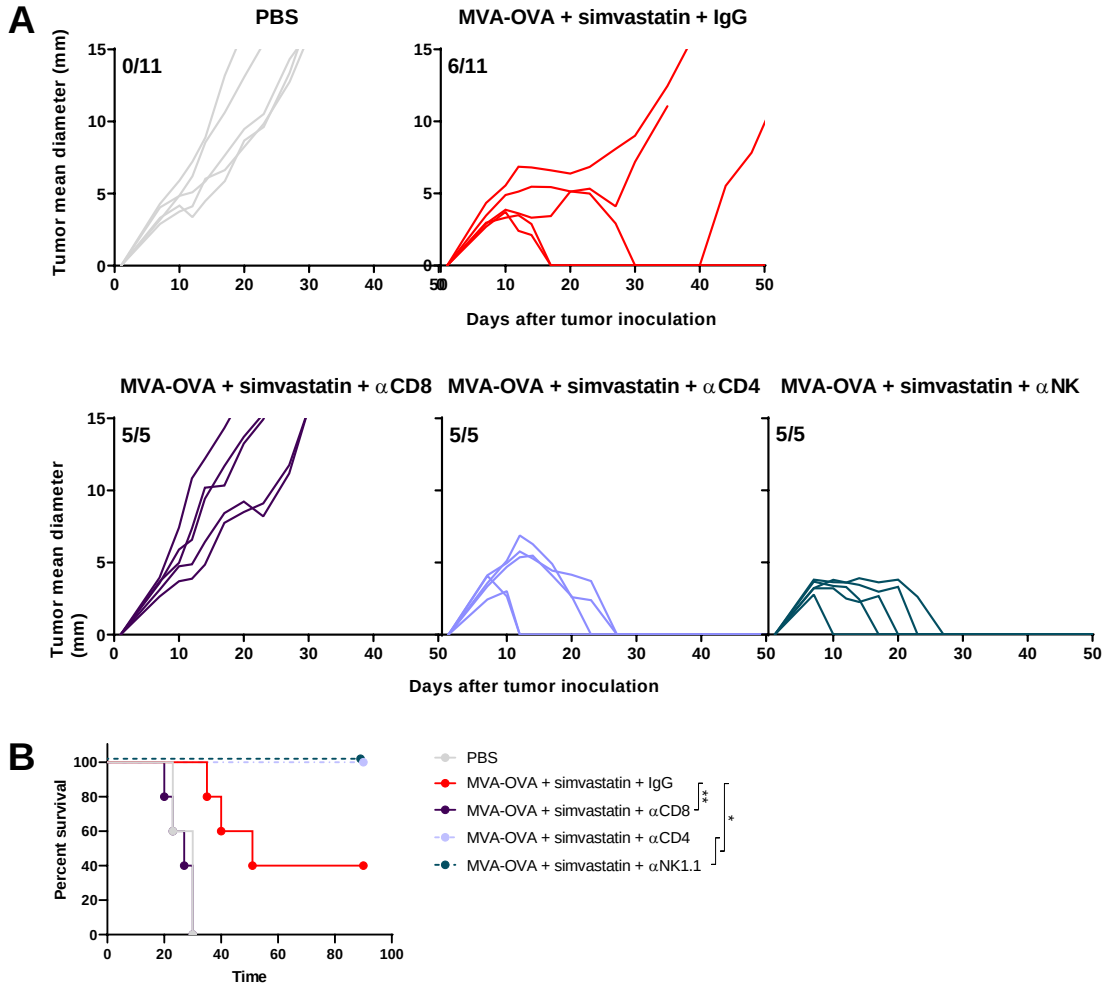

Figure 5. CD8$^+$ lymphocytes are required for the antitumor activity of MVA-OVA combined with simvastatin, but CD4+ lymphocytes and NK cells are detrimental. B16-OVA melanoma cells were injected subcutaneously. Seven and fourteen days later, mice were treated intraperitoneally with vehicle or simvastatin (20 µg/mice), after 2 hours, MVA-OVA ($5x10^7$ $TCID_{50}$ per mouse) was administered subcutaneously in the tumor area. Anti-CD8 mAb, anti-CD4 mAb or anti-NK1.1 (200 µg/mice) were administered intra-peritoneally one day before first therapeutic treatment administration and on days +2, +6, +9 and +13 **(A)** Individual follow-up of mean tumor diameters indicating the fraction of mice completely rejecting established tumors. **(B)** Overall

survival of the indicated treatment groups. Two-sided log-rank test. * $p<0.05$. ** $p<0.01$.

To further understand the impact of simvastatin on the antitumor effect of MVA-OVA, we used flow cytometry to evaluate the presence of different immune populations in cell suspensions from the tumor-draining lymph node and the tumor. B cells, $CD4^+$ lymphocytes, $CD8^+$ lymphocytes, and tumor-specific $CD8^+$ lymphocytes increased in the tumor-draining lymph node in those animals treated with MVA-OVA alone or with the combination (Figure 6A). However, a marked difference between both groups was observed in the tumor microenvironment. While MVA-OVA tended to decrease these immune populations as compared to PBS-treated mice, MVA-OVA combined with simvastatin dramatically increased the infiltration by B cells, $CD8^+$ T lymphocytes and tumor-specific $CD8^+$ T lymphocytes into the tumor microenvironment (Figure 6B).

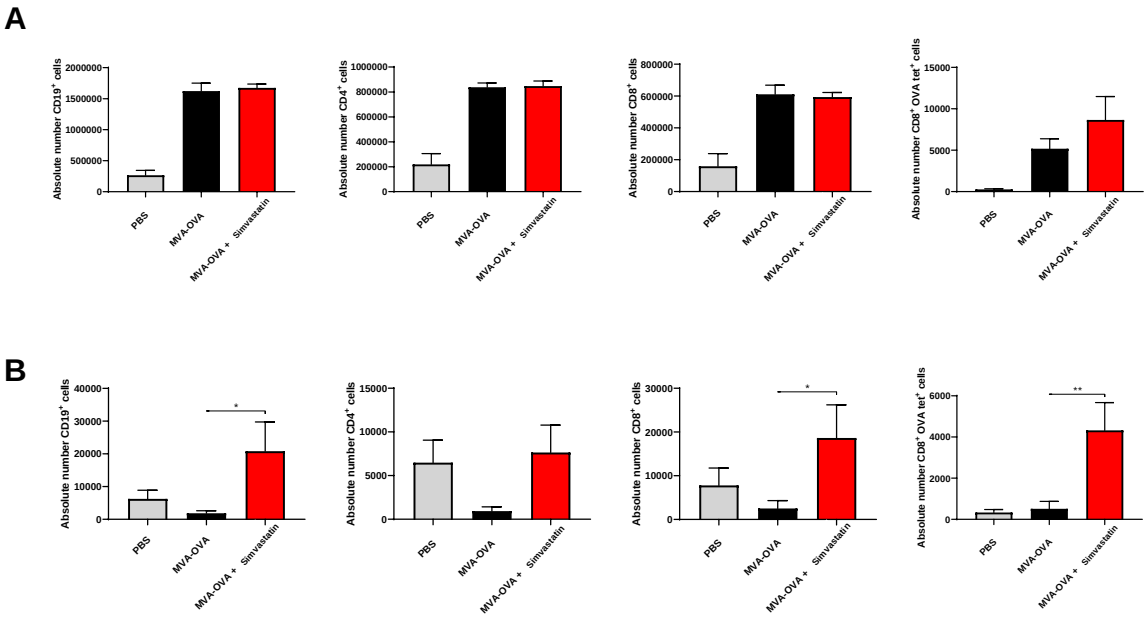

Figure 6. Lymphocyte changes in the tumor-draining lymph node and in the tumor microenvironment in response to MVA-OVA combined with simvastatin. B16-OVA melanoma cells were injected subcutaneously. Seven days later, mice were treated intraperitoneally with vehicle or simvastatin (20 µg/mice), after 2 hours, MVA-OVA ($5x10^7$ $TCID_{50}$ per mouse) was administered subcutaneously in the tumor area. Five days later, mice were sacrificed and immune cells in the tumor-draining lymph node and tumors were analyzed by flow cytometry. **(A)** The absolute number of $CD19^+$ cells, $CD4^+$ lymphocytes, $CD8^+$ lymphocytes, and OVA $tetramer^+$ $CD8^+$ lymphocytes in the draining lymph node. **(B)** As in A but in the tumor microenvironment. One-way ANOVA followed by Dunnett's post-test. * $p<0.05$, ** $p<0.01$.

Discussion

The discovery and development of monoclonal antibodies that block the PD1-PD-L1 pathway has demonstrated the clinical usefulness of the normalization of the immune response in the tumor microenvironment. Clinical response to these antibodies is characterized by long-term tumor growth control and manageable immune-related adverse effects (73). The discovery of this critical pathway paves the way for the clinical development of other cancer immunotherapies designed to enhance effector immune responses. Among these strategies, virotherapy has long been pursued in clinical trials, but approvals are limited to Talimogene Laherparepvec (74). We have focused our attention on modified vaccinia virus Ankara, a viral vector vaccine in clinical development as an anti-cancer drug. The attenuation process through the passage in chicken embryo fibroblasts led to the deletion of several soluble and intracellular factors that block the type I IFN response (75). Thus, MVA is able to induce the release of interferon-beta and alpha. Several genetic strategies have been developed to block MVA-mediated type I IFN expression but the safety of these MVA vectors for in vivo use might be compromised (75, 76). Here, we aimed to find a clinically available drug that might permit MVA expression and immunogenicity by transiently blocking the activity of type I IFN. We analyzed several compounds for their ability to reduce the surface levels of IFNR1 and to block clathrin-mediated endocytosis. Simvastatin and atorvastatin were able to decrease those processes and effectively attenuated type I IFN signaling. The maximum effect was achieved at 37.5 μM, a concentration that does not affect cell viability in the case of simvastatin. In the case of atorvastatin a concentration of 300 μM was required, and a slight reduction in the cell viability was observed. Based on this in vitro data, we selected simvastatin for *in vivo* experiments since the desired effect was achieved at a lower and safer

concentration. First, we evaluated whether the intraperitoneal administration of simvastatin reduced the interferon-stimulated genes (ISGs) four hours after intratumoral MVA-OVA administration. The type I IFN release mediated by MVA-OVA infection induced the activation of three ISGs. This effect was significantly blocked by the intraperitoneal administration of simvastatin in two out of three ISGs. The reduction of type I IFN signaling led to an improvement in the tumor control attained by MVA-OVA. This synergistic effect was independent of the route of simvastatin administration. Since the adjuvant effect mediated by the blockade of geranylgeranylation of Rab5 was only observed after intramuscular injection of simvastatin (68), we can exclude that this is the main mechanism of action in our system. The mechanism of action relies entirely on $CD8^+$ T lymphocytes according to depletion experiments. Interestingly, MVA-OVA reduced the tumor infiltration of immune cells, likely due to the cytotoxic activity of a high local concentration of type I IFN (38). Thus, transient type I IFN blockade may overcome this early detrimental effect, promoting tumor immune cell infiltration. Among these immune cells, a marked increase in tumor-specific T cell infiltration was observed that may explain the increased antitumor effect. In contrast to the beneficial effect of $CD8^+$ T lymphocytes, $CD4^+$ T lymphocytes and NK cells were detrimental for the final outcome of the combined treatment, although the mechanism is yet unclear. Both immune cell populations are potent producers of pro-inflammatory cytokines such as IFN-γ and TNF that might induce activation-induced cell death of effector $CD8^+$ T lymphocytes as has been previously reported for the combination of anti.CTLA-4 and anti-PD-1 monoclonal antibodies (77, 78). Depletion of Treg cells by anti-CD4 mAbs are also to be considered as a potential explanation. NK-cell lysis of $CD8^+$ lymphoblast undergoing activation could also be related to the observations following NK1.1 depletion.

In conclusion, we have identified and repurposed a clinically available drug that potentiates the antitumor effect of an MVA encoding a tumor-associated antigen. This is a feasible clinical intervention that may boost the clinical results of MVA-based vaccines in clinical trials.

Acknowledgments

This study was supported by Instituto de Salud Carlos III (PI16/00668 and PI19/01128) cofinanced by Fondos Feder and Joint Translational Call for Proposals 2015 (JTC 2015) TRANSCAN-2 (code: TRS-2016-00000371). S.T. received a grant from Gobierno de Navarra (code: 0011-1408-2016-000002).

Chapter 3 : “Scavenger receptor class B type I is required for 25-hydroxycholecalciferol cellular uptake and signaling in myeloid cells”

Title

Scavenger receptor class B type I is required for 25-hydroxycholecalciferol cellular uptake and signaling in myeloid cells

Authors

Shirley Tenesaca[1,2], Marcos Vasquez[1,2], Myriam Fernandez-Sendin[1,2], Claudia Augusta Di Trani[1,2], Nuria Ardaiz[1,2], Celia Gomar[1,2], Ignacio Melero[1,2,3,4], Pedro Berraondo[1,2,3,*]

Affiliations

[1]Program of Immunology and Immunotherapy, Cima Universidad de Navarra, Pamplona, Spain.

[2]Navarra Institute for Health Research (IDISNA), Pamplona, Spain.

[3]Centro de Investigación Biomédica en Red de Cáncer (CIBERONC), Spain.

[4]Department of Oncology, Clínica Universidad de Navarra, Pamplona, Spain

Abstract

Vitamin D_3 is a critical molecule for the properly controlled activity of the immune system. Vitamin D deficiency is a prevalent condition associated with an increased risk of autoimmune diseases and cancer due to the immune dysfunction associated with low levels of circulating 25-hydroxycholecalciferol (25(OH)D). Therapeutic strategies to restore the activity of vitamin D_3 will benefit from a more profound knowledge of the highly regulated vitamin D_3 system. Here, we describe a novel regulatory pathway of vitamin D_3 biology. Using a polyclonal antibody, two different chemical inhibitors, and high-density lipoprotein as a competing ligand, we demonstrate that the 25-hydroxycholecalciferol signaling pathway in myeloid cells depends on scavenger receptor class B type I (SR-B1). This effect was observed in the THP-1 monocytic cell line and in human primary monocytes. SR-B1 inhibition abrogates the cellular uptake of 25(OH)D leading to a general shut down of the gene transcription program modulated by 25(OH)D. The results obtained at the transcriptional level were confirmed at the protein level for CD14 in the THP-1 cell line. In conclusion, SR-B1 plays a critical role in vitamin D_3 biology, paving the way for novel therapeutic interventions.

Introduction

Vitamin D_3 is a family of steroid hormones derived from a cholesterol precursor. In animals, the most important sources of vitamin D_3 or cholecalciferol are the skin and diet. In a chemical reaction catalyzed by UV-B light, the cholesterol precursor 7-dehydrocholesterol is transformed into cholecalciferol. This form of vitamin D_3 has reduced biological activity and must be converted into the more active vitamin D_3 form 1,25-dihydroxycholecalciferol or calcitriol. This conversion occurs in two anatomically distant organs. First, cholecalciferol is converted into 25-hydroxycholecalciferol (25(OH)D) or calcidiol by the 25-hydroxylases (CYP2R1, CYP27A1, CYP3A4, and CYP2D5) present in the liver. The 25(OH)D is further hydroxylated by the enzyme 1-α-hydroxylase (Cyp27B1) expressed in the kidney and immune cells such as monocytes and macrophages to produce the active 1,25-dihydroxycholecalciferol. The liver step is not regulated, and the circulating levels of 25(OH)D reflect the dietary uptake and skin production of vitamin D_3 (79, 80). 25(OH)D circulates mainly bound to the vitamin D-binding protein (85%) or albumin (15%). Only 0.03% of 25(OH)D circulates freely (81). These complexes provide a long half-life in circulation of several weeks. In contrast, the half-life of the bioactive form lasts only hours and the production is highly regulated both in the kidney and in the innate immune cells by the inducers of the enzyme CYP27B1 (82).

The active 1,25-dihydroxycholecalciferol has a 500 times higher affinity than 25(OH)D to the vitamin D receptor (VDR) (83). The vitamin D receptor is present in the cytoplasm and, upon binding to vitamin D_3, is transported into the nucleus, forms heterodimers with the retinoid-X-receptor and then, is able to bind to the vitamin D response elements present in the promoter of the target genes (84). The modulation of the gene transcription is responsible for the biological activities of vitamin D_3 (85). This

hormone is critical for calcium, phosphate, and magnesium homeostasis and is therefore essential for bone homeostasis (79). Interestingly, the vitamin D receptor is expressed in most immune cells, and the expression of the Cyp27B1 enzyme can be induced in monocytes and macrophages. Vitamin D_3 also mediates important differentiation effects during the ontogeny of leukocytes from bone marrow precursors (86). Thus, these myeloid-derived cells are able to locally generate the bioactive form of vitamin D_3 that, upon interaction with the VDR, induce the production of the antimicrobial peptide cathelicidin. Cathelicidin is able to induce cytokine release by other immune cells as well as to kill bacteria and tumor cells. The induction of cathelicidin by vitamin D_3 is important for the immune response against tuberculosis and certain tumors such as lymphomas (87, 88). Interestingly, the antimicrobial peptide is also involved in the antibody-dependent cell cytotoxicity of rituximab mediated by macrophages (88).

Free circulating 25(OH)D is supposed to gain access to the cell cytoplasm by passive diffusion across the cell membrane (89), while the 25(OH)D bound to the vitamin D-binding protein is only able to enter cells that express megalin and cubilin such as the kidney, parathyroid gland, mammary cells and placenta (90-92).

In this work, we analyze the entry of 25(OH)D into human myeloid-derived cell lines and human monocytes. Interestingly, we describe that entry is dependent on the activity of scavenger receptor class B type I (SR-B1) and is decreased by the SR-B1 main ligand high-density lipoproteins (HDLs). SR-B1 is a membrane glycoprotein involved in cellular lipid exchange. It is expressed at low levels in most cells and is highly expressed in the liver and steroidogenic glands. SR-B1 binds multiple ligands such as high-density lipoproteins, low-density lipoproteins, very-low-density lipoproteins, serum amyloid A, lipopolysaccharides, Gram-negative and Gram-positive bacteria,

hepatitis C viruses and the *Plasmodium* parasite (93). Its role as an internalizing receptor for vitamin D is reported herein.

Experimental Section

Cell lines and culture media

The human mammary carcinoma cell line BT-474 was kindly donated by Dr. Miguel Lopez-Botet (Hospital del Mar, Barcelona, Spain) and the monocytic leukemia cell line THP-1 was obtained from ATCC (TIB-202). THP-1 were cultured in medium consisting of RPMI 1640 (Gibco, Karlsruhe, Germany) supplemented with 2 mM glutamine (Sigma–Aldrich, Taufkirchen, Germany), 100 IU penicillin, 100 µg/ml streptomycin (Gibco), and 10% (v/v) fetal bovine serum (FBS; Gibco) in a humidified incubator at 37°C and 5% CO_2. BT-474 were cultured in medium consisting of DMEM/F12 (Gibco) supplemented as RPMI 1640 with addition of phenol red 0.02 mM (Sigma-Aldrich, Steinheim, Germany). Human monocytes were purified from PBMCs from healthy donors using Miltenyi human CD14 MicroBeads and a Miltenyi AutoMACS magnetic cell separator (Miltenyi Biotech, Gladbach, Germany), according to the manufacturer's instructions.

Reagents

BLT-1 and 25(OH)D (Product number: H4014) were purchased from Sigma-Aldrich and were reconstituted in DMSO and ethanol, respectively. Human HDLs were purchased from RayBiotech Inc (Norcross, GA). SR-B1 antibody was acquired from Novus Biologicals (Product number: NB400-113) (Littleton, CO), 25-[26, 27-^{3}H] hydroxycholecalciferol was obtained from PerkinElmer (Spokane, WA); specific activity 10 µCi/ml, (5µCi in 500µl of toluene) and ITX 5061 was acquired from WuXi AppTec Co Ltd (Shanghai, China).

RNA isolation and quantification of mRNA.

RNA was isolated from studied cell lines and sorted $CD14^+$ monocytes using the Maxwell® 16 Total RNA Purification Kit (Promega, Madison, WI), quantified in a NanoDrop spectrophotometer (Thermo Scientific, Wilmington, DE), and retrotranscribed (300 ng) to cDNA with Moloney murine leukemia virus (M-MLV) reverse transcriptase from Promega, following the manufacturer's instructions.

Quantitative real-time PCR was performed with iQ SYBR Green Supermix (Bio-Rad, Hercules, CA) using specific primers for each gene, purchased from Invitrogen (Thermo Scientific). RLP0 5'-aacatctccccttctcctt-3' 5'-gaaggccttgacctttcag-3'; cathelicidin antimicrobial peptide (CAMP) 5'-tgggcctggtgatgcct-3' 5'-cgaaggacagcttccttgtagc3'; homo sapiens CD14 molecule (CD14), transcript variant 3 5'-gacctaaagataaccggcacc-3' 5'- gcaatgctcagtaccttgagg-3'; homo sapiens interleukin 1, beta (IL1B) 5'-atgatggcttattacagtggcaa-3' 5'-gtcggagattcgtagctgga-3'; homo sapiens heparin-binding EGF-like growth factor (HBEGF) 5'-atcgtggggcttctcatgttt-3' 5'-ttagtcatgcccaacttcacttt-3'. As RLP0 levels remained constant across different experimental conditions, this parameter was used to standardize gene expression. The amount of each transcript was expressed by the formula $2\Delta Ct$, with ct being the point at which the fluorescence rises significantly above background levels.

Inhibition assay

First, THP-1 cells (2.5×10^5 /well) were seeded in 96-well plates in triplicate in RPMI culture media without fetal bovine serum and treated with increasing amounts of

25(OH)D or vehicle for 24h. Then, RNA was isolated as described previously. Once the adequate amount of 25(OH)D corresponding to the maximum upregulation of CAMP mRNA levels was selected, THP-1 cells (2.5 $x10^5$ /well), BT-474 (1.0 $x10^5$ /well) and $CD14^+$ monocytes ($3.0x10^5$) were pretreated with SR-B1 antibody (1:125) or HDL 100 µg/ml for thirty minutes. After that, the cells were treated with 25(OH)D 100 nM or vehicle. BLT-1 (30µM) and ITX-5061 (5µM) were added simultaneously with 25(OH)D (100nM) and cells were incubated for 24 h and processed under the same conditions described above.

Gene Microarray

RNA was isolated from THP-1 cells using the Maxwell® 16 Total RNA Purification Kit (Promega) and quantified in a NanoDrop spectrophotometer (Thermo Scientific). Microarray analysis was performed using the Affymetrix platform at Bioinformatics Unit in the CIC-IBMCC. Labeling and hybridizations were performed according to protocols from Affymetrix (Santa Clara, CA). Briefly, 100 ng of total RNA were amplified and labeled using the WT Plus reagent kit (Affymetrix) and then hybridized to Clariom S human Array (Affymetrix). Washing and scanning were performed using GeneChip System of Affymetrix (GeneChip Hybridization Oven 645, GeneChip Fluidics Station 450 and GeneChip Scanner 7G).

Flow cytometry analysis

Flow cytometry analysis was performed using a FACS Canto II flow cytometer (BD Biosciences, San Diego, CA). First, THP-1 cells (2.5 $x10^5$ /well) were seeded in 96-well

plates in triplicate in RPMI culture media without fetal bovine serum and treated with 100 µM 25(OH)D, anti-SR-B1 polyclonal antibody (1:125) or both for 48 hours. Finally, THP-1 cells were harvested and were stained with anti-human CD14 APC-conjugated (18D11; ImmunoTools (Friesoythe, Germany)), Zombie NIR (Biolegend (San Diego, CA)) for 15 min at 4 °C in PBS, and then washed twice and resuspended in the same buffer for further flow cytometric analysis.

Effect of 25(OH)D on LPS activity

THP-1 cells (2.5 $x10^5$ /well) were seeded in 96-well plates in triplicate in RPMI culture media without fetal bovine serum and treated with 100 µM 25(OH)D, anti-SR-B1 polyclonal antibody (1:125) or both for 48 hours. Then, culture media was replaced with DMEM complete plus 5 ng/ml LPS and cells were incubated for 24 hours. Finally, IL-8 in the supernatants was determined by ELISA according to the manufacturer's instructions.

Cell uptake of tritium-labeled 25-hydroxycholecalciferol

THP-1 cells (5.0 $x10^5$ /well) were seeded in 24-well plates in RPMI 1640 10% FBS and were differentiated to macrophages with phorbol myristate acetate 5 ng/µl during 24 hours in a humidified incubator at 37°C and 5% CO_2. Cells were washed 3-5 times with serum-free RPMI and were treated with HDL 100µg/ml or SR-B1 antibody (1:320) for 30 minutes in serum-free RPMI. Then, cells were washed and 25-[26, 27-^{3}H]-hydroxicholecalciferol was added at a concentration of 0.02µCi/ml with or without HDL 100µg/ml or SR-B1 antibody (1:1000) in serum-free RPMI for 45 minutes. After

incubation, cells were washed 5 times with serum-free RPMI and lysed with 300 µl of RNA Lysis Buffer from Maxwell® 16 Total RNA Purification Kit. The lysed cell preparation (300 µl) was added to 4 ml scintillation fluid (Microscint TM Packard, Groningen, The Netherlands) for determination of radioactivity by scintillation counting, TopCount ® NXT Microplate Scintillation counter (Perkin-Elmer, Wellesley, MA).

Statistical analysis

GraphPad Prism version 8.2.1 software (GraphPad Software, Inc., San Diego, CA) was used for statistical analysis. Data were analyzed by one-way ANOVA followed by Dunnett's multiple comparisons test. P values <0.05 were considered to be statistically significant.

Results

25(OH)D-mediated induction of cathelicidin expression depends on scavenger receptor class B type 1.

Cathelicidin (CAMP) expression in macrophages is essential for the control of intracellular bacteria such as tuberculosis and is also a mediator of the antitumor activity of macrophages (88). Thus, we used the induction of the expression of the CAMP gene as a readout to explore the requirements for the action of 25(OH)D on myeloid-derived cells. The activity of this compound depends on intracrine activation of free 25(OH)D by Cyp27B1. Using the human monocytic cell line THP-1, we confirmed that free 25(OH)D was able to upregulate CAMP mRNA levels (Figure 1A). However, the activity of 25(OH)D was totally abrogated by pretreatment of the THP-1 cells with an anti-SR-B1 antibody (Figure 1B). This result challenges the accepted hypothesis that free 25(OH)D gains access to monocytes/macrophages by passive diffusion and suggests the control of vitamin D_3 immune activity by SR-B1 ligands. To address this issue, we analyzed the effect of the primary SR-B1 ligand, high-density lipoproteins (HDLs), on the immune activity of 25(OH)D. As expected by the involvement of SR-B1, HDLs incubation of THP-1 prevented the activity of 25(OH)D on the upregulation of CAMP mRNA levels (Figure 1B). To further corroborate the involvement of SR-B1 in 25(OH)D activity, we treated the THP-1 cells with two different chemical inhibitors specific for SR-B1: BLT-1 (94) and ITX-5061 (95). Both compounds inhibited the upregulation of CAMP transcripts induced by 25(OH)D (Figure 1C).

The role of SR-B1 in vitamin D biology was confirmed not only in human primary monocytes (Figure 1D) but also in a breast cancer cell line (Figure 1E). Cancer cells upregulate CAMP mRNA levels upon treatment with 25(OH)D, fostering invasion and

metastasis (96). Thus, SR-B1 mediates the uptake and activity of 25(OH)D both in myeloid-derived cells and tumor cells.

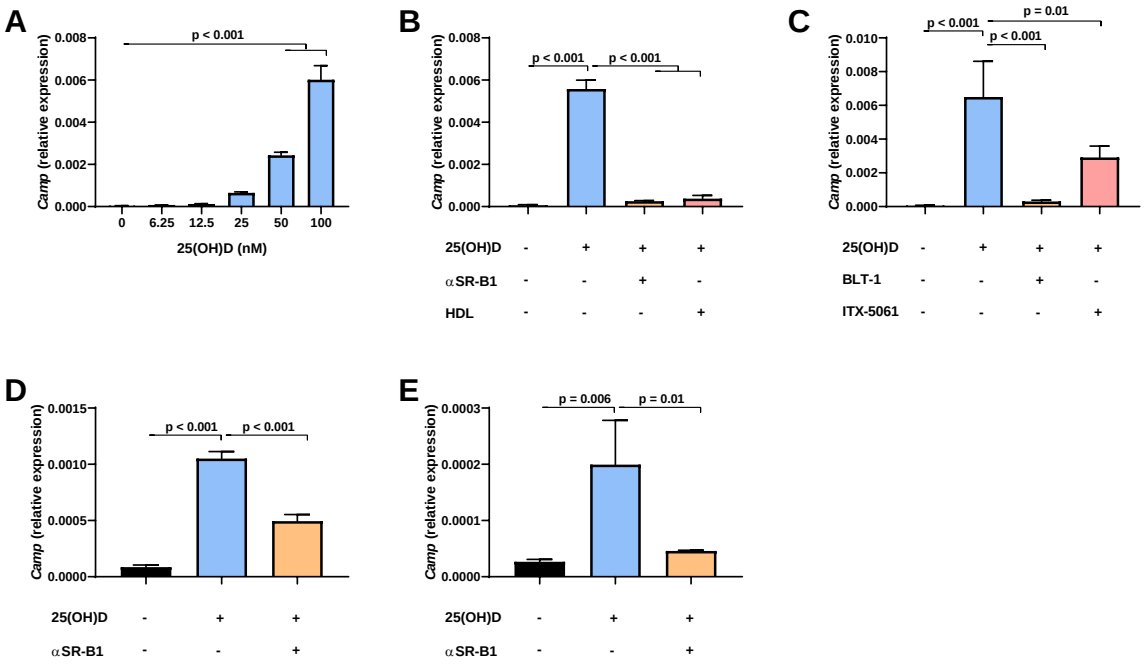

Figure 1. SR-B1 blockade abrogates 25(OH)D–mediated cathelicidin upregulation. **(A)** Cathelicidin mRNA levels were determined by real-time RT-PCR in 2.5 x 10^5 THP-1 cells treated for 24 hours with different doses of 25(OH)D. **(B)** Cathelicidin mRNA levels in 2.5 x 10^5 THP-1 cells pretreated for 30 minutes with SR-B1 blockade by anti-SR-B1 polyclonal antibody (1:125) or high-density lipoproteins (100 µg/ml) and treated 24 hours with 100 µM 25(OH)D **(C)** As in B but blocking SR-B1 with BLT-1 (30 µM) or ITX-5061 (5 µM). **(D)** Human monocytes purified with magnetic beads were stimulated with 100 µM 25(OH)D and SR-B1 was blocked by anti-SR-B1 polyclonal antibody (1:125). Cathelicidin mRNA levels were analyzed by real-time RT-PCR after 24 hours. **(E)** As in D but using BT474 human breast cancer cells.

Scavenger receptor class B type 1 mediates the internalization of 25(OH)D

The biological activity of 25(OH)D requires the internalization of the compound to the cytosol, where it is converted into 1,25-dihydroxycholecalciferol by Cyp27B1 present in the outer mitochondrial membrane and cytoplasm. Thus, we analyzed the entry of thymidine labeled 25(OH)D to confirm the involvement of SR-B1 in 25(OH)D internalization. Radioactivity incorporation was analyzed after incubation of THP-1 cells for 45 min. A strong signal was detected in control cells that was almost entirely abolished by incubation with anti-SR-B1 polyclonal antibody or HDLs (Figure 2).

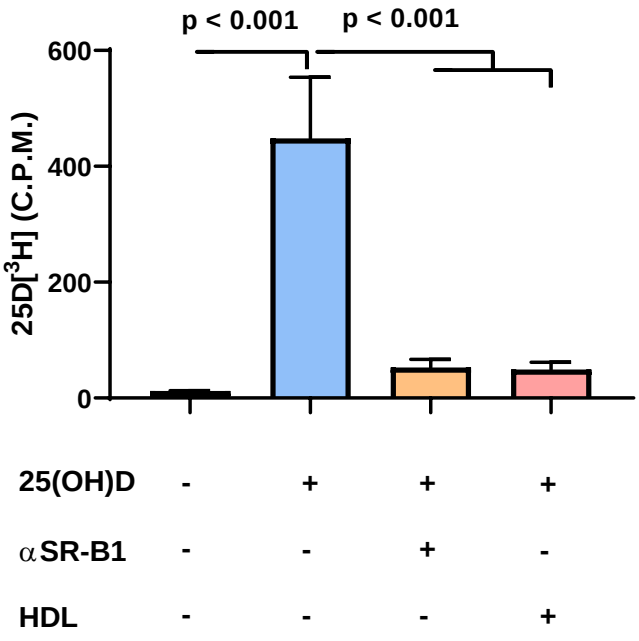

Figure 2. SR-B1 blockade abrogates 25(OH)D cellular uptake. A pretreatment with anti-SR-B1 polyclonal antibody (1:320) or HDL (100 µg/ml) was done for 30 minutes before the addition of thymidine labeled 25(OH)D. Internalization of thymidine labeled 25(OH)D was determined by liquid scintillation 45 minutes after incubation of 5.0 x10^5 THP-1 cells with 25-[26,27-^{3}H]-hydroxycholecalciferol (0.02µCi/ml) with or without SR-B1 blockade by anti-SR-B1 polyclonal antibody (1:1000) or high-density lipoproteins (100 µg/ml).

Global suppression of 25(OH)D gene modulation by anti-SR-B1 polyclonal antibody

We next performed gene expression profiling to exclude the possibility that SR-B1 affects just a fraction of 25(OH)D-modulated genes. For this analysis, we established a cut off value for the expression log ratio of 0.8. Figure 3A represents the normalized expression of each transcript between 0 to 1. 25(OH)D induced the expression over this cut off value in 75 genes while decreased the expression value in 68 transcripts. The effect of 25(OH)D on these transcript levels was abolished by cotreatment with anti-SR-B1 antibody in the vast majority of transcripts. Indeed, the expression pattern of these vitamin D-modulated transcripts in cells treated with 25(OH)D and anti-SR-B1 antibody was similar to the expression pattern observed in cells treated with the anti-SR-B1 antibody alone (Figure 3A). Only 13 transcripts were up- or down-regulated in both experimental conditions treated with 25(OH)D. A similar number, sixteen, of commonly modulated transcripts were observed in the group treated with 25(OH)D alone and in the group treated with anti-SR-B1 antibody alone (Figure 3B). To validate the gene expression profiling data, we selected three of the most upregulated transcripts in response to 25(OH)D treatment: *CD14*, *IL1B,* and *HBEGF*. The mRNA levels of these transcripts were analyzed by real-time PCR in THP-1 cells treated with anti-SR-B1 antibody, 25(OH)D or both. The mRNA levels of the three transcripts was highly upregulated by vitamin D treatment, and the expression returned to baseline levels when the 25(OH)D was combined with anti-SR-B1 antibody (Figure 3C). Thus, these results support the hypothesis that SR-B1 is essential for 25(OH)D uptake since an overall abrogation of the effect of 25(OH)D on gene expression profiling was observed.

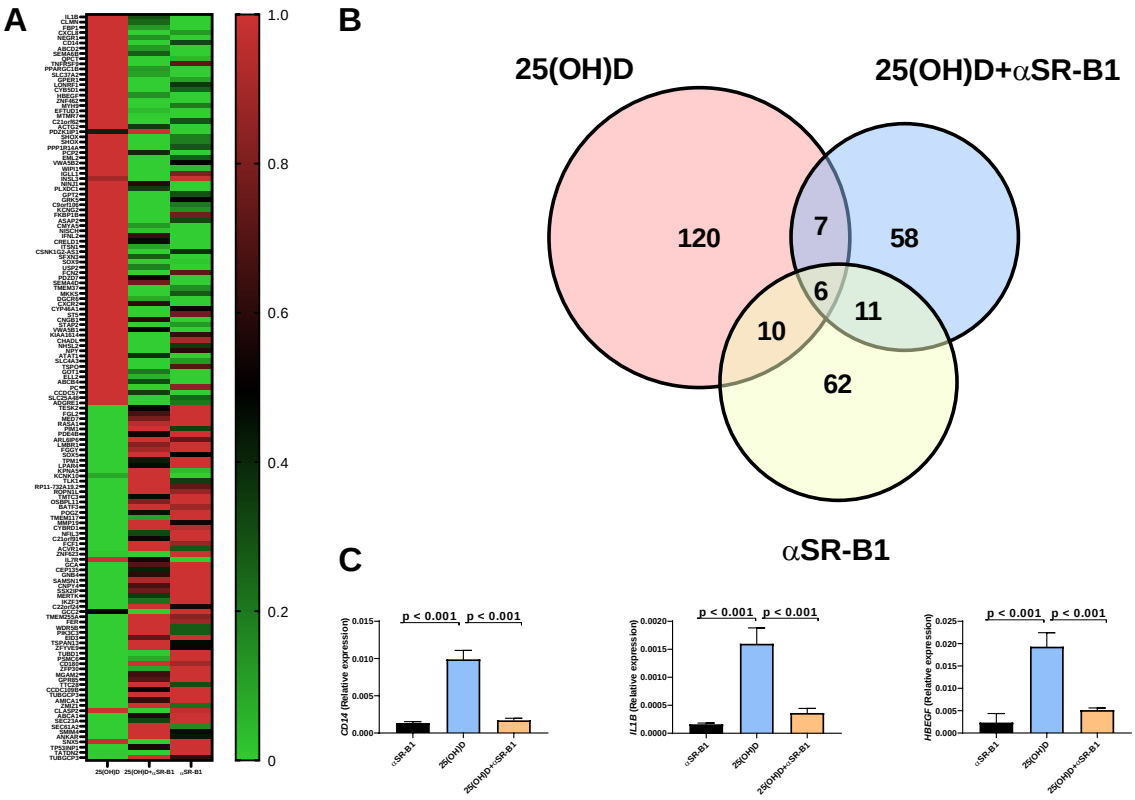

Figure 3. SR-B1 blockade abrogates 25(OH)D–mediated gene expression. 2.5 x 10^5 THP-1 cells were pretreated with +/- anti-SR-B1 polyclonal antibody (1:125) for 30 minutes. Then, cells were treated with 100 µM 25(OH)D and 24 hours later, overall gene expression was analyzed by Affymetrix platform**. (A)** Heat-map representing the gene modulated by 25(OH)D with a 0.8 cut-off value. **(B)** Venn diagram representing the number of different transcripts modulated by 25(OH)D alone, 25(OH)D plus anti-SR-B1 antibody or anti-SR-B1 alone with a 0.8 cut-off value. **(C)** Real-time RT-PCR of *CD14*, *IL1B* and *HBEGF* transcripts in THP-1 cells incubated for 24 hours with 100 µM 25(OH)D with or without anti-SR-B1 polyclonal antibody (1:125).

Induction of cell surface levels of CD14 by 25(OH)D *is blocked by an anti-SR-B1 antibody*

Next, we focused our attention on CD14, one of the transcripts that increased in the gene expression array and was validated by real-time PCR. CD14 is a monocyte marker with an important role as co-receptor of lipopolysaccharide. Moreover, the induction of this monocyte marker upon vitamin D administration has been well-established [19]. In line with this report, 48 hours after 25(OH)D treatment, CD14 protein levels as analyzed by flow cytometry increased dramatically. However, the co-treatment with an anti-SR-B1 antibody avoided the 25(OH)D effect on cell surface CD14 (Figure 4A and B). To further corroborate the implications of CD14 modulation, we stimulated with lipopolysaccharide THP-1 cells pretreated with 25(OH)D in the presence or absence of anti-SR-B1 antibody. IL-8 release was used as a read out of the lipopolysaccharide activity on this monocytic cell line. In line with the cell surface levels of CD14, IL-8 release was increased in cells pretreated with 25(OH)D but not in those cells pretreated with the combination of 25(OH)D plus anti-SR-B1 antibody (Figure 4C).

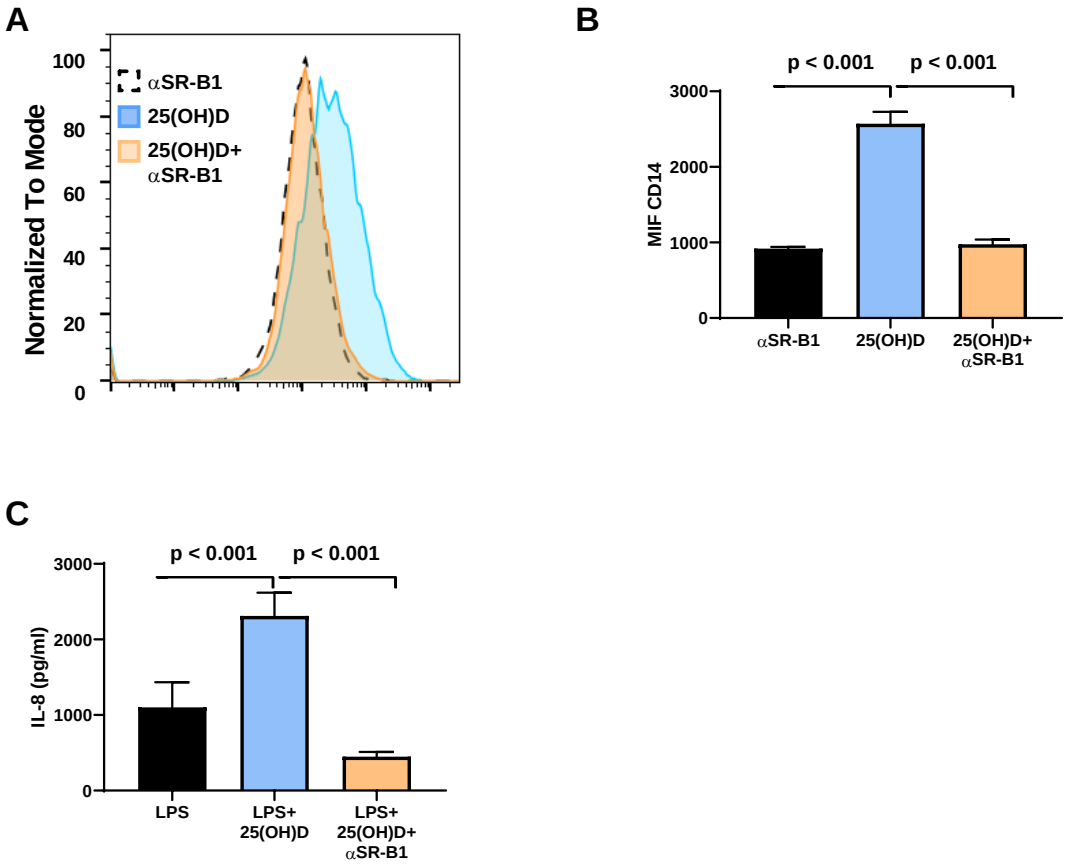

Figure 4. SR-B1 blockade abrogates 25(OH)D-induced CD14 protein level. THP-1 cells were treated with 100 µM 25(OH)D with or without anti-SR-B1 polyclonal antibody (1:125). **(A, B)** Fourty-eight hours later, CD14 protein level was determined by flow cytometry. **(C)** Fourty-eight hours later, DMEM complete plus 5ng/ml LPS was added for 24 hours, then IL-8 ELISA of supernatants was performed.

Discussion

Vitamin D_3 deficiency is a major public health problem. Rickets is the extreme manifestation of vitamin D_3 deficiency, but a plethora of other chronic diseases is statistically associated with low circulating 25(OH)D levels. Among these diseases, the most relevant are osteoporosis, cancer, autoimmune diseases and cardiovascular diseases (79). To prevent the consequences of vitamin D_3 deficiency, different vitamin D supplementation strategies have been implemented. These range from administration of high dose vitamin D over-the-counter formulations to food supplementation. Vitamin D intestinal absorption is an active process mediated by cholesterol transporters such as SR-B1 (97). Based on this report, we hypothesized that this receptor may be also relevant for the cellular uptake of 25(OH)D. Our data demonstrate that SR-B1 is an essential receptor for cellular 25(OH)D uptake and signaling. The cellular activity of 25(OH)D is abolished by four different SR-B1 blocking molecules: a polyclonal antibody, two different chemical inhibitors, and the major endogenous ligand, high-density lipoprotein. Vitamin D_3 bioactivity is tightly regulated at different levels. Skin and diet inactive forms of vitamin D are metabolized in the liver to generate the main circulating form of vitamin D_3, 25(OH)D. This form with intermediate activity is converted into the more active form of vitamin D_3, 1,25-dihydroxycholecalciferol in tissues that express the enzyme 1α-hydroxylase such as the kidney. In addition, most circulating 25(OH)D is bound to vitamin D binding protein, yielding a significant pool of inactive circulating vitamin D. Finally, the enzyme vitamin D_3-24-hydroxylase (CYP24) limits the activity of both 25(OH)D, and 1,25-dihydroxycholecalciferol. This enzyme catabolizes both vitamin D forms into inactive calcitroic acid. Thus, the vitamin D_3 system is complex and highly regulated (80). Here, we show an additional control mechanism of this complex system: the cross-talk between SR-B1 ligands and vitamin

D activity. Based on these findings, free 25(OH)D will remain unable to interact the cytosolic vitamin D receptors in anatomical locations with high concentration of SR-B1 ligands while 25(OH)D will become available for cell uptake in tissue areas with low concentration of lipoproteins due to reduced blood perfusion. For instance, monocytes in circulation will not be activated by 25(OH)D but macrophages infiltrating the tumor microenvironment will be the main target of the active and available 25(OH)D. The results may also be implicated in the relationship between 25(OH)D and circulating levels of high-density lipoprotein. High-density lipoprotein cholesterol and size of high-density lipoproteins are significantly higher in subjects with adequate circulating levels of 25(OH)D (98, 99). Interestingly, levels of this vitamin D_3 form were not correlated with other markers of cardiovascular disease such as blood pressure, glucose, or other serum lipid markers (99). Since we have demonstrated that vitamin D and high-density lipoprotein compete for the same receptor, it is reasonable to hypothesize that increased circulating levels of vitamin D will increase the half-life in circulation of high-density lipoprotein as well as enhancing cell production due to increased apolipoprotein A-1 synthesis (100-104).

In conclusion, we demonstrate that SR-B1 participates in the cellular uptake of 25(OH)D. Thus, SR-B1 is not only a novel regulatory protein in vitamin D_3 bioactivity but is also a novel target to design a vitamin D variant with enhanced bioactivity.

Acknowledgements

This study was supported by Instituto de Salud Carlos III (PI16/00668) cofinanced by Fondos Feder and Joint Translational Call for Proposals 2015 (JTC 2015) TRANSCAN-2 (code: TRS-2016-00000371). S.T. received a grant from Gobierno de Navarra (code: 0011-1408-2016-000002).

GENERAL DISCUSSION

Type I IFNs (IFNs) are among the most pleiotropic cytokines and are produced and sensed by almost every cell type in the body. IFNs activate intracellular antimicrobial programs and influence the development of innate and adaptive immune responses. Canonical type I IFN signaling activates the Janus kinase (JAK)–signal transducer and activator of transcription (STAT) pathway, leading to transcription of IFN-stimulated genes (ISGs) (105).

The dysregulation of IFNs production and function mediates immune pathogenesis, such as inflammatory autoimmune diseases and infectious diseases via aberrant activation of inflammatory responses or suppressing immune responses to pathogens. Thus, IFN responses need to be tightly regulated to achieve protective immunity against microbial infection while avoiding harmful toxicity caused by inappropriate or prolonged IFN signaling (106).

The discovery of type I IFN role in cancer immune surveillance at first, and cancer immune editing later, made these cytokines and the immune sensing networks that drive their production very attractive for more in-depth investigation in preclinical and clinical contexts (107).

In this Ph.D. project, I have exploited the beneficial role of type I IFN in different indications.

The first work aimed to exploit the upregulation of suppressor cells and molecules such as PD-1 and interleukin 10 on $CD8^+$ T lymphocytes that were observed in a tumor model after sustained delivery of IFN-α or IFN-α fused to apolipoprotein A-1 by an adeno-associated vector. A model of experimental autoimmune encephalomyelitis (EAE) was chosen because it is mediated by autoantigen-specific T cells dependent on critical costimulatory signals for their full activation and regulation (108). It has been

reported that the programmed death-1 (PD-1) costimulatory pathway plays a critical role in regulating peripheral tolerance in murine EAE and appears to be a major contributor to the resistance of disease induction in CD28-deficient mice (109). In addition, reportedly, IL-10 plays a more critical role in the regulation of EAE by regulating autopathogenic Th1 responses (110).

Our work has demonstrated the protective action of low and sustained IFN-α in an EAE model. The mechanism of action involves several immune cells. First, sustained levels of IFN-α generated by AAV-IFN-α induced the upregulation of Ly6C surface expression in the monocytic population. This result is in line with a report that showed that IFN signaling is involved in $Ly6C^{hi}$ monocyte generation (111, 112). Second, we identified a T regulatory cell (Treg) expansion. Accordingly, a recent study demonstrates that myeloma cells drive Treg expansion and activation by secreting type 1 interferon (113). Finally, we observed that splenocytes from AAV-IFN-α groups up-regulated the expression of immunosuppressive molecules such as interleukin 10, indoleamine-2,5-dioxygenase, and programmed death 1. Moreover, the neutrophil presence was reduced, and $CD4^+$ T cells showed reduced intracellular levels of cytokines such as IL-17A and IFN-γ. This immunomodulation recapitulates some of the effects produced by recombinant IFN-β therapy in multiple sclerosis patients. Several studies have proposed possible mechanisms underlying the therapeutic response to rIFNβ. Reports indicated that recombinant IFN-β improves suppressive immune activities (114), inhibits interferon gamma-induced class II major histocompatibility complex expression by certain cell types (115), inhibits mitogen-driven T-cell activation (116), decreases proinflammatory cytokine production such as interferon-gamma and tumor necrosis factor (117).

The second study of this Ph.D. project identified a novel strategy to improve the antitumor activity of oncolytic viruses by inhibiting transiently IFNAR receptor and ISGs expression. The right choice of an experimental model was required to demonstrate this concept. We selected a cancer vaccine based on a viral vector encoding a tumor-associated antigen to promote the strong activation of cytotoxic T cells (CTLs). Viral vaccine technology provides danger signals for the activation of the immune response since virus infection is sensed by a variety of cellular pattern-recognition receptors and triggers the synthesis of interferons, which are secreted by the infected cells (118). Indeed, delivery of an antigen without appropriate co-stimulatory signals results in T cell ignorance, T cell anergy, or even T cell deletion. In this case, the selected vaccine was the modified vaccinia virus Ankara (MVA), which preferentially targets antigen-presenting cells (119) and is a potent inducer of type I IFN in conventional dendritic cells and tumor cells (120).

Beneficial effects IFN-α for the stimulation of the immune response are well known. It has been stated that type I IFN positively regulates T cell activation, clonal expansion, memory cell differentiation and survival in response to viral infection (121-123). Additionally, it is known that type I IFN regulates dendritic cell function (124-126), essential for antigen-specific T cell activation. A recent study suggests that type I IFN is critical in the regulation of the key CTL effector granzyme B expression and tumor growth control *in vivo* (127).

Almost all viruses have evolved mechanisms to defend themselves against the interferon system to avoid extinction. It has been reported that vaccinia E3L protein masks the sensitivity of vaccinia virus to ISG15. Moreover, after infection with wild type vaccinia virus, ISG15 was induced but did not form conjugates. Thus the antiviral activity of ISG15 conjugation was annulled (128). However, interestingly it was

suggested that ISG15 is involved in more functions than ISGylation. Absence of intracellular ISG15 in the patients' cells prevented the accumulation of USP18, a potent negative regulator of IFN-α/β signaling, resulting in the enhancement and amplification of IFN-α/β responses (129). All these immune evasion mechanisms have been eliminated during the generation of MVA and therefore, MVA may benefit from strategies to transiently block the IFN signaling. In this work, we report that statins temporarily inhibit the activity of the IFNAR1 receptor and therefore, the production of ISGs such as ISG15, USP18, and 2,5 OAS. These results are in line with a report that shows that high-dose add-on statin therapy significantly reduces IFN-β function and type 1 interferon responses in relapsing-remitting MS patients (130). The transient blockade of IFNAR receptor and ISGs production in a mouse model of B16-OVA melanoma treated with an MVA vaccine causes an improvement in the tumor growth control. These results can be explained by an increment of tumor-specific CD8 T lymphocytes. It is likely that the combination of statins and MVA allows an improvement in the timing of the exposition of type I interferon to the immune cells.

In consequence, we observed a more robust expansion of T lymphocytes. Recently, it was demonstrated that the massive expansion of antigen-specific CD8 T cells that occurs in response to viral infection is critically dependent on the direct action of type I interferons on $CD8^+$ T cells. In this report, it was shown that the lack of direct $CD8^+$ T cell contact with type I IFN causes a reduction in their capacity to expand and generate memory cells (128). In conclusion, the combination of statins and MVA limits the antiviral effect of type I IFN and the initial phase of the vaccination, while promotes the beneficial type I IFN on the effector immune cells in a second phase of the viral vaccine.

In the last work included in this Ph.D. project, we analyzed the effect of SR-B1 blockade of the biological activity of vitamin D. Our findings support that 25-hydroxycholecalciferol is selectively uptake by SR-B1 in myeloid cells. This receptor is strategically positioned in the plasma membrane for regulating the influx and efflux of cholesteryl esters, free cholesterol, and related lipids into and out of the cell. SR-B1 has a particular conformation to allow a hydrophobic channel, which enables the function of SR-B1. Moreover, there are strong structural similarities between cholesterol and vitamin D that justify the use of the same receptor. Vitamin D is a steroid-like hormone. It is synthesized by several steps from 7-dehydrocholesterol after exposure to ultraviolet irradiation in the skin (131). In addition, 7-dehydrocholesterol can be converted to cholesterol in the Kandutsch-Russell pathway by the enzyme 7-dehydrocholesterol reductase (DHCR7) (132). Therefore, cholesterol and vitamin D are nearly identical in chemical structure.

Some studies support the cross-talk between 25-hydroxyvitamin D and HDL cholesterol levels. Jorde et al. (133), who conducted one of the most extensive observational studies (n = 17411) analyzing the associations between 25(OH)D and serum lipid profiles in a general population, reported significant positive correlations of 25(OH)D with LDL-cholesterol, HDL- cholesterol, and total cholesterol. The analysis demonstrated that high serum 25(OH)D levels are associated with high serum LDL- cholesterol, HDL-cholesterol, and total cholesterol levels, and with low serum triglyceride levels. Another study in pregnant women that evaluated total and free 25(OH)D reported a significant positive correlation between total 25(OH)D and HDL. Nevertheless, in this study LDL showed no associations with total 25(OH)D but significant inverse relations with free 25(OH)D (134).

Finally, a study demonstrated that vitamin D intestinal absorption is an active process mediated by cholesterol transporters such as SR-B1. Interestingly, when competition assays were performed, cholecalciferol uptake was reduced in the presence of cholesterol and tocopherol, suggesting common absorption pathways for the three molecules (97). Therefore, simply passive diffusion of 25(OH)D is not coherent with these results but points to a controlled uptake.

Vitamin D has emerged as an important regulator of the immune system. This regulation is mediated through interference with nuclear transcription factors such as NFAT and NF-κB or by direct interaction with vitamin D responsive elements in the promoter regions of cytokine genes (135). Interestingly, the VDR is constitutively expressed by antigen-presenting cells such as macrophages and dendritic cells and its expression is inducible in lymphocytes following activation (135). In humans, the hormone-bound VDR directly induces the transcription of genes encoding antimicrobial peptides, pattern recognition receptors and key cytokines implicated in innate immune responses (136). Relevantly, toll-like receptor activation of human macrophages enhances expression of CYP27B1 and VDR, leading to the induction of the antimicrobial peptide cathelicidin under conditions of 25(OH)D sufficiency (137). Therefore, innate immune cells respond to pathogen threats by becoming responsive to endogenous levels of 25(OH)D and producing a VDR-driven innate immune response.

CD14 expression is strongly induced by 1,25(OH)2D3 in human monocytes, which exhibit increased adherence to endothelial cells during inflammation and respond to LPS during bacterial infection (138-140). It also stimulates the release of IL-1β in a dose-dependent manner (141). It is well known that monocytes and macrophages are producers of IL-1β in response to infectious or other stressful events and initiates a potent defensive inflammatory response (142). It has been reported that vitamin D_3 also

induced an increase in heparin-binding epidermal growth factor–like growth factor (HB-EGF) transcripts by primary leukemic cells. Heparin-binding epidermal growth factor–like growth factor (HB-EGF) is an EGF family member expressed by numerous cell types that bind to EGF receptor 1 (HER-1) or 4 (HER-4) inducing mitogenic and/or chemotactic activities (143).

Epidemiological studies have shown that 25OHD deficiency is closely associated with common chronic diseases such as bone metabolic disorders, tumors, cardiovascular diseases, and diabetes. 25OHD deficiency is also a risk factor for neuropsychiatric disorders and autoimmune diseases (144). Additionally, vitamin D deficiency is common in breast cancer patients, and some evidence suggests that low vitamin D status enhances the risk for disease development or progression. Studies have demonstrated that vitamin receptor activation in breast tumor leads to inhibition of cell cycle, induction of cell death and induction of differentiation. Detailed analysis of the cell death process revealed that both apoptosis and autophagy are induced by 1,25(OH)2D3 and/or synthetic VDR agonists in breast cancer cells *in vitro* (145). Consequently, comprehension of vitamin D uptake mechanisms will help to find new targets to treat cancer.

CONCLUSIONS

1. The sustained delivery of low-dose interferon-alpha or interferon-alpha fused to apolipoprotein A-1 improved the therapeutical activity of recombinant interferon-alpha for the treatment of the experimental autoimmune encephalomyelitis by immune cell remodeling.

2. Statins are potent interferon-alpha inhibitors due to their ability to reduce the membrane levels of the interferon-alpha/beta receptor and to reduce endocytosis.

3. Simvastatin enhanced the antitumor activity of a modified vaccinia virus Ankara encoding ovalbumin in B16-OVA tumor-bearing mice.

4. The antitumor effect of the combination of simvastatin and modified vaccinia virus Ankara encoding ovalbumin depends critically on $CD8^+$ T lymphocytes.

5. The scavenger receptor class B type 1 mediated the cellular uptake of 25-hydroxycholecalciferol in myeloid cells.

BIBLIOGRAPHY

1. Rankin LC, Artis D. Beyond Host Defense: Emerging Functions of the Immune System in Regulating Complex Tissue Physiology. Cell. 2018;173:554-67.

2. Eberl G. Immunity by equilibrium. Nature reviews Immunology. 2016;16(8):524-32.

3. Seager RJ, Hajal C, Spill F, Kamm RD, Zaman MH. Dynamic interplay between tumour, stroma and immune system can drive or prevent tumour progression. Convergent Science Physical Oncology. 2017;3:034002.

4. Lu K-L, Wu M-Y, Wang C-H, Wang C-W, Hung S-I, Chung W-H, et al. The Role of Immune Checkpoint Receptors in Regulating Immune Reactivity in Lupus. Cells. 2019;8:1213.

5. Pecht I. Immuno-receptors: from recognition to signaling and function. European Biophysics Journal. 2018;47:363-71.

6. Chen Daniel S, Mellman I. Oncology Meets Immunology: The Cancer-Immunity Cycle. Immunity. 2013;39:1-10.

7. Dunn GP, Old LJ, Schreiber RD. The Immunobiology of Cancer Immunosurveillance and Immunoediting. Immunity. 2004;21:137-48.

8. Whiteside TL, Demaria S, Rodriguez-Ruiz ME, Zarour HM, Melero I. Emerging Opportunities and Challenges in Cancer Immunotherapy. Clinical cancer research : an official journal of the American Association for Cancer Research. 2016;22(8):1845-55.

9. Fioravanti J, Medina-Echeverz J, Berraondo P. Scavenger receptor class B, type I: a promising immunotherapy target. Immunotherapy. 2011;3:395-406.

10. Vasquez M, Simões I, Consuegra-Fernández M, Aranda F, Lozano F, Berraondo P. Exploiting scavenger receptors in cancer immunotherapy: Lessons from CD5 and SR-B1. European journal of immunology. 2017;47:1108-18.

11. Vasquez M, Fioravanti J, Aranda F, Paredes V, Gomar C, Ardaiz N, et al. Interferon alpha bioactivity critically depends on Scavenger receptor class B type I function. Oncoimmunology. 2016;5:1-13.

12. Vasquez M, Paredes-Cervantes V, Aranda F, Ardaiz N, Gomar C, Berraondo P. Antitumor effect of an adeno-associated virus expressing apolipoprotein A-1 fused to interferon alpha in an interferon alpha-resistant murine tumor model. Oncotarget. 2017;8:5247-55.

13. Asano L, Watanabe M, Ryoden Y, Usuda K, Yamaguchi T, Khambu B, et al. Vitamin D Metabolite, 25-Hydroxyvitamin D, Regulates Lipid Metabolism by Inducing Degradation of SREBP/SCAP. Cell chemical biology. 2017;24(2):207-17.

14. Reich DS, Lucchinetti CF, Calabresi PA. Multiple Sclerosis. The New England journal of medicine. 2018;378(2):169-80.

15. Gajofatto A, Benedetti MD. Treatment strategies for multiple sclerosis: When to start, when to change, when to stop? World journal of clinical cases. 2015;3(7):545-55.

16. Platanias LC. Mechanisms of type-I- and type-II-interferon-mediated signalling. Nature reviews Immunology. 2005;5(5):375-86.

17. Kieseier BC. The mechanism of action of interferon-beta in relapsing multiple sclerosis. CNS drugs. 2011;25(6):491-502.

18. Durelli L, Bongioanni MR, Cavallo R, Ferrero B, Ferri R, Ferrio MF, et al. Chronic systemic high-dose recombinant interferon alfa-2a reduces exacerbation rate, MRI signs of disease activity, and lymphocyte interferon gamma production in relapsing-remitting multiple sclerosis. Neurology. 1994;44(3 Pt 1):406-13.

19. Magyari M, Bach Sondergaard H, Sellebjerg F, Soelberg Sorensen P. Preserved in vivo response to interferon-alpha in multiple sclerosis patients with neutralising

antibodies against interferon-beta (REPAIR study). Multiple sclerosis and related disorders. 2013;2(2):141-6.

20. Squillacote D, Martinez M, Sheremata W. Natural alpha interferon in multiple sclerosis: results of three preliminary series. The Journal of international medical research. 1996;24(3):246-57.

21. Schreiber G, Piehler J. The molecular basis for functional plasticity in type I interferon signaling. Trends in immunology. 2015;36(3):139-49.

22. Severson C, Hafler DA. T-cells in multiple sclerosis. Results and problems in cell differentiation. 2010;51:75-98.

23. Dos Passos GR, Sato DK, Becker J, Fujihara K. Th17 Cells Pathways in Multiple Sclerosis and Neuromyelitis Optica Spectrum Disorders: Pathophysiological and Therapeutic Implications. Mediators of inflammation. 2016;2016:5314541.

24. Venken K, Hellings N, Liblau R, Stinissen P. Disturbed regulatory T cell homeostasis in multiple sclerosis. Trends in molecular medicine. 2010;16(2):58-68.

25. Zhang X, Koldzic DN, Izikson L, Reddy J, Nazareno RF, Sakaguchi S, et al. IL-10 is involved in the suppression of experimental autoimmune encephalomyelitis by CD25+CD4+ regulatory T cells. International immunology. 2004;16(2):249-56.

26. Kohm AP, Carpentier PA, Anger HA, Miller SD. Cutting edge: CD4+CD25+ regulatory T cells suppress antigen-specific autoreactive immune responses and central nervous system inflammation during active experimental autoimmune encephalomyelitis. Journal of immunology. 2002;169(9):4712-6.

27. Kavrochorianou N, Markogiannaki M, Haralambous S. IFN-beta differentially regulates the function of T cell subsets in MS and EAE. Cytokine & growth factor reviews. 2016;30:47-54.

28. Zettl UK, Hecker M, Aktas O, Wagner T, Rommer PS. Interferon beta-1a and beta-1b for patients with multiple sclerosis: updates to current knowledge. Expert review of clinical immunology. 2018;14(2):137-53.

29. Panitch H, Goodin DS, Francis G, Chang P, Coyle PK, O'Connor P, et al. Randomized, comparative study of interferon beta-1a treatment regimens in MS: The EVIDENCE Trial. Neurology. 2002;59(10):1496-506.

30. Sharief MK. Dose and Frequency of Administration of Interferon-beta Affect its Efficacy in Multiple Sclerosis. Clinical drug investigation. 2003;23(9):551-9.

31. Rothuizen LE, Buclin T, Spertini F, Trinchard I, Munafo A, Buchwalder PA, et al. Influence of interferon beta-1a dose frequency on PBMC cytokine secretion and biological effect markers. Journal of neuroimmunology. 1999;99(1):131-41.

32. Williams GJ, Witt PL. Comparative study of the pharmacodynamic and pharmacologic effects of Betaseron and AVONEX. Journal of interferon & cytokine research : the official journal of the International Society for Interferon and Cytokine Research. 1998;18(11):967-75.

33. Witt PL, Storer BE, Bryan GT, Brown RR, Flashner M, Larocca AT, et al. Pharmacodynamics of biological response in vivo after single and multiple doses of interferon-beta. Journal of immunotherapy with emphasis on tumor immunology : official journal of the Society for Biological Therapy. 1993;13(3):191-200.

34. Randomised double-blind placebo-controlled study of interferon beta-1a in relapsing/remitting multiple sclerosis. PRISMS (Prevention of Relapses and Disability by Interferon beta-1a Subcutaneously in Multiple Sclerosis) Study Group. Lancet. 1998;352(9139):1498-504.

35. Evidence of interferon beta-1a dose response in relapsing-remitting MS: the OWIMS Study. The Once Weekly Interferon for MS Study Group. Neurology. 1999;53(4):679-86.

36. Cocco E, Marchi P, Floris G, Mascia MG, Deriu M, Sirca A, et al. Effect of dose and frequency of interferon beta-1a administration on clinical and magnetic resonance imaging parameters in relapsing-remitting multiple sclerosis. Functional neurology. 2006;21(3):145-9.

37. Mingozzi F, High KA. Therapeutic in vivo gene transfer for genetic disease using AAV: progress and challenges. Nature reviews Genetics. 2011;12(5):341-55.

38. Fioravanti J, Gonzalez I, Medina-Echeverz J, Larrea E, Ardaiz N, Gonzalez-Aseguinolaza G, et al. Anchoring interferon alpha to apolipoprotein A-I reduces hematological toxicity while enhancing immunostimulatory properties. Hepatology. 2011;53(6):1864-73.

39. Melendez-Torres GJ, Armoiry X, Court R, Patterson J, Kan A, Auguste P, et al. Comparative effectiveness of beta-interferons and glatiramer acetate for relapsing-remitting multiple sclerosis: systematic review and network meta-analysis of trials including recommended dosages. BMC neurology. 2018;18(1):162.

40. Reuss R. PEGylated interferon beta-1a in the treatment of multiple sclerosis - an update. Biologics : targets & therapy. 2013;7:131-8.

41. Hamana A, Takahashi Y, Tanioka A, Nishikawa M, Takakura Y. Amelioration of Experimental Autoimmune Encephalomyelitis in Mice by Interferon-Beta Gene Therapy, Using a Long-Term Expression Plasmid Vector. Molecular pharmaceutics. 2017;14(4):1212-7.

42. Hartemann A, Bensimon G, Payan CA, Jacqueminet S, Bourron O, Nicolas N, et al. Low-dose interleukin 2 in patients with type 1 diabetes: a phase 1/2 randomised,

double-blind, placebo-controlled trial. The lancet Diabetes & endocrinology. 2013;1(4):295-305.

43. Lim TY, Martinez-Llordella M, Kodela E, Gray E, Heneghan MA, Sanchez-Fueyo A. Low-Dose Interleukin-2 for Refractory Autoimmune Hepatitis. Hepatology. 2018;68(4):1649-52.

44. Jiang L, Berraondo P, Jerico D, Guey LT, Sampedro A, Frassetto A, et al. Systemic messenger RNA as an etiological treatment for acute intermittent porphyria. Nature medicine. 2018.

45. Pastor F, Berraondo P, Etxeberria I, Frederick J, Sahin U, Gilboa E, et al. An RNA toolbox for cancer immunotherapy. Nature reviews Drug discovery. 2018;17(10):751-67.

46. Alvarez-Sola G, Uriarte I, Latasa MU, Fernandez-Barrena MG, Urtasun R, Elizalde M, et al. Fibroblast growth factor 15/19 (FGF15/19) protects from diet-induced hepatic steatosis: development of an FGF19-based chimeric molecule to promote fatty liver regeneration. Gut. 2017;66(10):1818-28.

47. Golding A, Rosen A, Petri M, Akhter E, Andrade F. Interferon-alpha regulates the dynamic balance between human activated regulatory and effector T cells: implications for antiviral and autoimmune responses. Immunology. 2010;131(1):107-17.

48. Metidji A, Rieder SA, Glass DD, Cremer I, Punkosdy GA, Shevach EM. IFN-alpha/beta receptor signaling promotes regulatory T cell development and function under stress conditions. Journal of immunology. 2015;194(9):4265-76.

49. Chen M, Chen G, Deng S, Liu X, Hutton GJ, Hong J. IFN-beta induces the proliferation of CD4+CD25+Foxp3+ regulatory T cells through upregulation of GITRL

on dendritic cells in the treatment of multiple sclerosis. Journal of neuroimmunology. 2012;242(1-2):39-46.

50. Bacher N, Raker V, Hofmann C, Graulich E, Schwenk M, Baumgrass R, et al. Interferon-alpha suppresses cAMP to disarm human regulatory T cells. Cancer research. 2013;73(18):5647-56.

51. Andtbacka RH, Kaufman HL, Collichio F, Amatruda T, Senzer N, Chesney J, et al. Talimogene Laherparepvec Improves Durable Response Rate in Patients With Advanced Melanoma. Journal of clinical oncology : official journal of the American Society of Clinical Oncology. 2015;33(25):2780-8.

52. Lichty BD, Breitbach CJ, Stojdl DF, Bell JC. Going viral with cancer immunotherapy. Nature reviews Cancer. 2014;14(8):559-67.

53. Meyer H, Sutter G, Mayr A. Mapping of deletions in the genome of the highly attenuated vaccinia virus MVA and their influence on virulence. The Journal of general virology. 1991;72 (Pt 5):1031-8.

54. Dai P, Wang W, Yang N, Serna-Tamayo C, Ricca JM, Zamarin D, et al. Intratumoral delivery of inactivated modified vaccinia virus Ankara (iMVA) induces systemic antitumor immunity via STING and Batf3-dependent dendritic cells. Science immunology. 2017;2(11).

55. Gulley JL, Borre M, Vogelzang NJ, Ng S, Agarwal N, Parker CC, et al. Phase III Trial of PROSTVAC in Asymptomatic or Minimally Symptomatic Metastatic Castration-Resistant Prostate Cancer. Journal of clinical oncology : official journal of the American Society of Clinical Oncology. 2019;37(13):1051-61.

56. Akira S, Uematsu S, Takeuchi O. Pathogen recognition and innate immunity. Cell. 2006;124(4):783-801.

57. Corrales L, Gajewski TF. Endogenous and pharmacologic targeting of the STING pathway in cancer immunotherapy. Cytokine. 2016;77:245-7.

58. Hervas-Stubbs S, Riezu-Boj JI, Gonzalez I, Mancheno U, Dubrot J, Azpilicueta A, et al. Effects of IFN-alpha as a signal-3 cytokine on human naive and antigen-experienced CD8(+) T cells. European journal of immunology. 2010;40(12):3389-402.

59. Berraondo P, Sanmamed MF, Ochoa MC, Etxeberria I, Aznar MA, Perez-Gracia JL, et al. Cytokines in clinical cancer immunotherapy. British journal of cancer. 2019;120(1):6-15.

60. Stark GR, Kerr IM, Williams BR, Silverman RH, Schreiber RD. How cells respond to interferons. Annual review of biochemistry. 1998;67:227-64.

61. Kurokawa C, Iankov ID, Anderson SK, Aderca I, Leontovich AA, Maurer MJ, et al. Constitutive Interferon Pathway Activation in Tumors as an Efficacy Determinant Following Oncolytic Virotherapy. Journal of the National Cancer Institute. 2018;110(10):1123-32.

62. Jackson JD, Markert JM, Li L, Carroll SL, Cassady KA. STAT1 and NF-kappaB Inhibitors Diminish Basal Interferon-Stimulated Gene Expression and Improve the Productive Infection of Oncolytic HSV in MPNST Cells. Molecular cancer research : MCR. 2016;14(5):482-92.

63. Patel MR, Jacobson BA, Ji Y, Drees J, Tang S, Xiong K, et al. Vesicular stomatitis virus expressing interferon-beta is oncolytic and promotes antitumor immune responses in a syngeneic murine model of non-small cell lung cancer. Oncotarget. 2015;6(32):33165-77.

64. Alain T, Lun X, Martineau Y, Sean P, Pulendran B, Petroulakis E, et al. Vesicular stomatitis virus oncolysis is potentiated by impairing mTORC1-dependent

type I IFN production. Proceedings of the National Academy of Sciences of the United States of America. 2010;107(4):1576-81.

65. Selman M, Ou P, Rousso C, Bergeron A, Krishnan R, Pikor L, et al. Dimethyl fumarate potentiates oncolytic virotherapy through NF-kappaB inhibition. Science translational medicine. 2018;10(425).

66. Dornan MH, Krishnan R, Macklin AM, Selman M, El Sayes N, Son HH, et al. First-in-class small molecule potentiators of cancer virotherapy. Scientific reports. 2016;6:26786.

67. Chow SC. Immunomodulation by statins: mechanisms and potential impact on autoimmune diseases. Archivum immunologiae et therapiae experimentalis. 2009;57(4):243-51.

68. Xia Y, Xie Y, Yu Z, Xiao H, Jiang G, Zhou X, et al. The Mevalonate Pathway Is a Druggable Target for Vaccine Adjuvant Discovery. Cell. 2018;175(4):1059-73 e21.

69. Berraondo P, Nouze C, Preville X, Ladant D, Leclerc C. Eradication of large tumors in mice by a tritherapy targeting the innate, adaptive, and regulatory components of the immune system. Cancer research. 2007;67(18):8847-55.

70. Marchetti M, Monier MN, Fradagrada A, Mitchell K, Baychelier F, Eid P, et al. Stat-mediated signaling induced by type I and type II interferons (IFNs) is differentially controlled through lipid microdomain association and clathrin-dependent endocytosis of IFN receptors. Molecular biology of the cell. 2006;17(7):2896-909.

71. Piehler J, Thomas C, Garcia KC, Schreiber G. Structural and dynamic determinants of type I interferon receptor assembly and their functional interpretation. Immunological reviews. 2012;250(1):317-34.

72. Vasquez M, Fioravanti J, Aranda F, Paredes V, Gomar C, Ardaiz N, et al. Interferon alpha bioactivity critically depends on Scavenger receptor class B type I function. Oncoimmunology. 2016;5(8):e1196309.

73. Sanmamed MF, Chen L. A Paradigm Shift in Cancer Immunotherapy: From Enhancement to Normalization. Cell. 2018;175(2):313-26.

74. Harrington K, Freeman DJ, Kelly B, Harper J, Soria JC. Optimizing oncolytic virotherapy in cancer treatment. Nature reviews Drug discovery. 2019;18(9):689-706.

75. Waibler Z, Anzaghe M, Frenz T, Schwantes A, Pohlmann C, Ludwig H, et al. Vaccinia virus-mediated inhibition of type I interferon responses is a multifactorial process involving the soluble type I interferon receptor B18 and intracellular components. Journal of virology. 2009;83(4):1563-71.

76. Sliva K, Martin J, von Rhein C, Herrmann T, Weyrich A, Toda M, et al. Interference with SAMHD1 restores late gene expression of modified vaccinia virus Ankara (MVA) in human dendritic cells and abrogates type I interferon expression. Journal of virology. 2019.

77. Perez-Ruiz E, Minute L, Otano I, Alvarez M, Ochoa MC, Belsue V, et al. Prophylactic TNF blockade uncouples efficacy and toxicity in dual CTLA-4 and PD-1 immunotherapy. Nature. 2019;569(7756):428-32.

78. Pai CS, Huang JT, Lu X, Simons DM, Park C, Chang A, et al. Clonal Deletion of Tumor-Specific T Cells by Interferon-gamma Confers Therapeutic Resistance to Combination Immune Checkpoint Blockade. Immunity. 2019;50(2):477-92 e8.

79. Holick MF. Vitamin D deficiency. The New England journal of medicine. 2007;357(3):266-81.

80. Bouillon R, Okamura WH, Norman AW. Structure-function relationships in the vitamin D endocrine system. Endocrine reviews. 1995;16(2):200-57.

81. Bikle DD, Schwartz J. Vitamin D Binding Protein, Total and Free Vitamin D Levels in Different Physiological and Pathophysiological Conditions. Frontiers in endocrinology. 2019;10:317.

82. Lips P. Relative value of 25(OH)D and 1,25(OH)2D measurements. Journal of bone and mineral research : the official journal of the American Society for Bone and Mineral Research. 2007;22(11):1668-71.

83. Rowling MJ, Gliniak C, Welsh J, Fleet JC. High dietary vitamin D prevents hypocalcemia and osteomalacia in CYP27B1 knockout mice. The Journal of nutrition. 2007;137(12):2608-15.

84. Mangelsdorf DJ, Evans RM. The RXR heterodimers and orphan receptors. Cell. 1995;83(6):841-50.

85. Pike JW, Meyer MB. The vitamin D receptor: new paradigms for the regulation of gene expression by 1,25-dihydroxyvitamin D(3). Endocrinology and metabolism clinics of North America. 2010;39(2):255-69, table of contents.

86. Hewison M. Vitamin D and the immune system: new perspectives on an old theme. Endocrinology and metabolism clinics of North America. 2010;39(2):365-79, table of contents.

87. Liu PT, Stenger S, Li H, Wenzel L, Tan BH, Krutzik SR, et al. Toll-like receptor triggering of a vitamin D-mediated human antimicrobial response. Science. 2006;311(5768):1770-3.

88. Bruns H, Buttner M, Fabri M, Mougiakakos D, Bittenbring JT, Hoffmann MH, et al. Vitamin D-dependent induction of cathelicidin in human macrophages results in cytotoxicity against high-grade B cell lymphoma. Science translational medicine. 2015;7(282):282ra47.

89. Jorde R. The Role of Vitamin D Binding Protein, Total and Free 25-Hydroxyvitamin D in Diabetes. Frontiers in endocrinology. 2019;10:79.

90. Chun RF, Lauridsen AL, Suon L, Zella LA, Pike JW, Modlin RL, et al. Vitamin D-binding protein directs monocyte responses to 25-hydroxy- and 1,25-dihydroxyvitamin D. The Journal of clinical endocrinology and metabolism. 2010;95(7):3368-76.

91. Nykjaer A, Dragun D, Walther D, Vorum H, Jacobsen C, Herz J, et al. An endocytic pathway essential for renal uptake and activation of the steroid 25-(OH) vitamin D3. Cell. 1999;96(4):507-15.

92. Rowling MJ, Kemmis CM, Taffany DA, Welsh J. Megalin-mediated endocytosis of vitamin D binding protein correlates with 25-hydroxycholecalciferol actions in human mammary cells. The Journal of nutrition. 2006;136(11):2754-9.

93. Fioravanti J, Medina-Echeverz J, Berraondo P. Scavenger receptor class B, type I: a promising immunotherapy target. Immunotherapy. 2011;3(3):395-406.

94. Nieland TJ, Penman M, Dori L, Krieger M, Kirchhausen T. Discovery of chemical inhibitors of the selective transfer of lipids mediated by the HDL receptor SR-BI. Proceedings of the National Academy of Sciences of the United States of America. 2002;99(24):15422-7.

95. Zhu H, Wong-Staal F, Lee H, Syder A, McKelvy J, Schooley RT, et al. Evaluation of ITX 5061, a scavenger receptor B1 antagonist: resistance selection and activity in combination with other hepatitis C virus antivirals. The Journal of infectious diseases. 2012;205(4):656-62.

96. Weber G, Chamorro CI, Granath F, Liljegren A, Zreika S, Saidak Z, et al. Human antimicrobial protein hCAP18/LL-37 promotes a metastatic phenotype in breast cancer. Breast cancer research : BCR. 2009;11(1):R6.

97. Reboul E, Goncalves A, Comera C, Bott R, Nowicki M, Landrier JF, et al. Vitamin D intestinal absorption is not a simple passive diffusion: evidences for involvement of cholesterol transporters. Molecular nutrition & food research. 2011;55(5):691-702.

98. Kazlauskaite R, Powell LH, Mandapakala C, Cursio JF, Avery EF, Calvin J. Vitamin D is associated with atheroprotective high-density lipoprotein profile in postmenopausal women. Journal of clinical lipidology. 2010;4(2):113-9.

99. Alkhatatbeh MJ, Amara NA, Abdul-Razzak KK. Association of 25-hydroxyvitamin D with HDL-cholesterol and other cardiovascular risk biomarkers in subjects with non-cardiac chest pain. Lipids in health and disease. 2019;18(1):27.

100. Jaimungal S, Wehmeier K, Mooradian AD, Haas MJ. The emerging evidence for vitamin D-mediated regulation of apolipoprotein A-I synthesis. Nutrition research. 2011;31(11):805-12.

101. Barbarawi M, Kheiri B, Zayed Y, Barbarawi O, Dhillon H, Swaid B, et al. Vitamin D Supplementation and Cardiovascular Disease Risks in More Than 83000 Individuals in 21 Randomized Clinical Trials: A Meta-analysis. JAMA cardiology. 2019.

102. Filgueiras MS, Suhett LG, Silva MA, Rocha NP, de Novaes JF. Lower vitamin D intake is associated with low HDL cholesterol and vitamin D insufficiency/deficiency in Brazilian children. Public health nutrition. 2018;21(11):2004-12.

103. Tavakoli F, Namakin K, Zardast M. Vitamin D Supplementation and High-Density Lipoprotein Cholesterol: A Study in Healthy School Children. Iranian journal of pediatrics. 2016;26(4):e3311.

104. Iqbal AM, Dahl AR, Lteif A, Kumar S. Vitamin D Deficiency: A Potential Modifiable Risk Factor for Cardiovascular Disease in Children with Severe Obesity. Children. 2017;4(9).

105. Ivashkiv LB, Donlin LT. Regulation of type I interferon responses. Nature reviews Immunology. 2014;14:36-49.

106. Chen K, Liu J, Cao X. Regulation of type I interferon signaling in immunity and inflammation: A comprehensive review. 2017.

107. Musella M, Manic G, Maria RD, Vitale I, Sistigu A. Type-I-interferons in infection and cancer: Unanticipated dynamics with therapeutic implications. Oncoimmunology. 2017;6.

108. Jiang Z, Li H, Fitzgerald DC, Zhang G-X, Rostami A. MOG(35-55) i.v suppresses experimental autoimmune encephalomyelitis partially through modulation of Th17 and JAK/STAT pathways. European journal of immunology. 2009;39:789-99.

109. Salama AD, Chitnis T, Imitola J, Ansari MJI, Akiba H, Tushima F, et al. Critical Role of the Programmed Death-1 (PD-1) Pathway in Regulation of Experimental Autoimmune Encephalomyelitis. The Journal of experimental medicine. 2003;198:71-8.

110. Bettelli E, Das MP, Howard ED, Weiner HL, Sobel RA, Kuchroo VK. IL-10 is critical in the regulation of autoimmune encephalomyelitis as demonstrated by studies of IL-10- and IL-4-deficient and transgenic mice. Journal of immunology (Baltimore, Md : 1950). 1998;161:3299-306.

111. Lee PY, Li Y, Kumagai Y, Xu Y, Weinstein JS, Kellner ES, et al. Type I interferon modulates monocyte recruitment and maturation in chronic inflammation. The American journal of pathology. 2009;175:2023-33.

112. Seo SU, Kwon HJ, Ko HJ, Byun YH, Seong BL, Uematsu S, et al. Type I interferon signaling regulates Ly6C(hi) monocytes and neutrophils during acute viral pneumonia in mice. PLoS pathogens. 2011;7(2):e1001304.

113. Kawano Y, Zavidij O, Park J, Moschetta M, Kokubun K, Mouhieddine TH, et al. Blocking IFNAR1 inhibits multiple myeloma–driven Treg expansion and immunosuppression. Journal of Clinical Investigation. 2018;128:2487-99.

114. Noronha A, Toscas A, Jensen MA. Interferon beta augments suppressor cell function in multiple sclerosis. Annals of neurology. 1990;27(2):207-10.

115. Ransohoff RM, Devajyothi C, Estes ML, Babcock G, Rudick RA, Frohman EM, et al. Interferon-beta specifically inhibits interferon-gamma-induced class II major histocompatibility complex gene transcription in a human astrocytoma cell line. Journal of neuroimmunology. 1991;33(2):103-12.

116. Rudick RA, Carpenter CS, Cookfair DL, Tuohy VK, Ransohoff RM. In vitro and in vivo inhibition of mitogen-driven T-cell activation by recombinant interferon beta. Neurology. 1993;43(10):2080-7.

117. Durelli L, Bongioanni MR, Cavallo R, Ferrero B, Ferri R, Verdun E, et al. Interferon alpha treatment of relapsing-remitting multiple sclerosis: long-term study of the correlations between clinical and magnetic resonance imaging results and effects on the immune function. Multiple sclerosis. 1995;1 Suppl 1:S32-7.

118. Fensterl V, Chattopadhyay S, Sen GC. No Love Lost Between Viruses and Interferons. 2015.

119. Altenburg AF, van de Sandt CE, Li BWS, MacLoughlin RJ, Fouchier RAM, van Amerongen G, et al. Modified Vaccinia Virus Ankara Preferentially Targets Antigen Presenting Cells In Vitro, Ex Vivo and In Vivo. Scientific reports. 2017;7:8580.

120. Dai P, Wang W, Yang N, Serna-Tamayo C, Ricca JM, Zamarin D, et al. Intratumoral delivery of inactivated modified vaccinia virus Ankara (iMVA) induces systemic antitumor immunity via STING and Batf3-dependent dendritic cells. Science immunology. 2017;2.

121. Le Bon A, Durand V, Kamphuis E, Thompson C, Bulfone-Paus S, Rossmann C, et al. Direct stimulation of T cells by type I IFN enhances the CD8+ T cell response during cross-priming. Journal of immunology. 2006;176(8):4682-9.

122. Kolumam GA, Thomas S, Thompson LJ, Sprent J, Murali-Krishna K. Type I interferons act directly on CD8 T cells to allow clonal expansion and memory formation in response to viral infection. The Journal of experimental medicine. 2005;202(5):637-50.

123. Marrack P, Kappler J, Mitchell T. Type I interferons keep activated T cells alive. The Journal of experimental medicine. 1999;189(3):521-30.

124. Tzeng A, Kauke MJ, Zhu EF, Moynihan KD, Opel CF, Yang NJ, et al. Temporally Programmed CD8alpha(+) DC Activation Enhances Combination Cancer Immunotherapy. Cell reports. 2016;17(10):2503-11.

125. Schiavoni G, Mattei F, Gabriele L. Type I Interferons as Stimulators of DC-Mediated Cross-Priming: Impact on Anti-Tumor Response. Frontiers in immunology. 2013;4:483.

126. Fuertes MB, Kacha AK, Kline J, Woo SR, Kranz DM, Murphy KM, et al. Host type I IFN signals are required for antitumor CD8+ T cell responses through CD8{alpha}+ dendritic cells. The Journal of experimental medicine. 2011;208(10):2005-16.

127. Lu C, Klement JD, Ibrahim ML, Xiao W, Redd PS, Nayak-Kapoor A, et al. Type I interferon suppresses tumor growth through activating the STAT3-granzyme B

pathway in tumor-infiltrating cytotoxic T lymphocytes. Journal for ImmunoTherapy of Cancer. 2019;7:157.

128. Kolumam GA, Thomas S, Thompson LJ, Sprent J, Murali-Krishna K. Type I interferons act directly on CD8 T cells to allow clonal expansion and memory formation in response to viral infection. The Journal of experimental medicine. 2005;202:637.

129. Zhang X, Bogunovic D, Payelle-Brogard B, Francois-Newton V, Speer SD, Yuan C, et al. Human intracellular ISG15 prevents interferon-α/β over-amplification and auto-inflammation. Nature. 2015;517:89-93.

130. Feng X, Han D, Kilaru BK, Franek BS, Niewold TB, Reder AT. Inhibition of interferon-beta responses in multiple sclerosis immune cells associated with high-dose statins. Archives of neurology. 2012;69(10):1303-9.

131. Holick MF, MacLaughlin JA, Clark MB, Holick SA, Potts JT, Anderson RR, et al. Photosynthesis of previtamin D3 in human skin and the physiologic consequences. Science (New York, NY). 1980;210:203-5.

132. Prabhu AV, Luu W, Li D, Sharpe LJ, Brown AJ. DHCR7: A vital enzyme switch between cholesterol and vitamin D production. Progress in Lipid Research. 2016;64:138-51.

133. Jorde R, Grimnes G. Exploring the association between serum 25-hydroxyvitamin D and serum lipids—more than confounding? European Journal of Clinical Nutrition. 2018;72:526-33.

134. Tsuprykov O, Buse C, Skoblo R, Hocher B. Comparison of free and total 25-hydroxyvitamin D in normal human pregnancy. The Journal of steroid biochemistry and molecular biology. 2019;190:29-36.

135. Etten Ev, Mathieu C. Immunoregulation by 1,25-dihydroxyvitamin D3: Basic concepts. The Journal of steroid biochemistry and molecular biology. 2005;97:93-101.

136. Dimitrov V, White JH. Species-specific regulation of innate immunity by vitamin D signaling. The Journal of steroid biochemistry and molecular biology. 2016;164:246-53.

137. Liu PT, Stenger S, Li H, Wenzel L, Tan BH, Krutzik SR, et al. Toll-Like Receptor Triggering of a Vitamin D-Mediated Human Antimicrobial Response. Science. 2006;311:1770-3.

138. Beekhuizen H, Blokland I, Corsèl-van Tilburg AJ, Koning F, van Furth R. CD14 contributes to the adherence of human monocytes to cytokine-stimulated endothelial cells. Journal of immunology (Baltimore, Md : 1950). 1991;147:3761-7.

139. Oberg F, Botling J, Nilsson K. Functional antagonism between vitamin D3 and retinoic acid in the regulation of CD14 and CD23 expression during monocytic differentiation of U-937 cells. Journal of immunology (Baltimore, Md : 1950). 1993;150:3487-95.

140. Wright S, Ramos R, Tobias P, Ulevitch R, Mathison J. CD14, a receptor for complexes of lipopolysaccharide (LPS) and LPS binding protein. Science. 1990;249:1431-3.

141. Tulk SE, Liao K-C, Muruve DA, Li Y, Beck PL, MacDonald JA. Vitamin D ₃ Metabolites Enhance the NLRP3-Dependent Secretion of IL-1β From Human THP-1 Monocytic Cells. Journal of Cellular Biochemistry. 2015;116:711-20.

142. Madej MP, Töpfer E, Boraschi D, Italiani P. Different Regulation of Interleukin-1 Production and Activity in Monocytes and Macrophages: Innate Memory as an Endogenous Mechanism of IL-1 Inhibition. Frontiers in pharmacology. 2017;8:335.

143. Vinante F, Rigo A, Papini E, Cassatella MA, Pizzolo G. Heparin-Binding Epidermal Growth Factor–Like Growth Factor/Diphtheria Toxin Receptor Expression by Acute Myeloid Leukemia Cells. Blood. 1999;93:1715-23.

144. Wang H, Chen W, Li D, Yin X, Zhang X, Olsen N, et al. Vitamin D and Chronic Diseases. Aging and disease. 2017;8:346-53.

145. Welsh J. Vitamin D and breast cancer_ Past and present. 2017.

ANNEX